THE SOUTHERN HEMISPHERE VLBI EXPERIMENT

ROBERT A. PRESTON
Jet Propulsion Laboratory, California Institute of Technology, Pasadena, California 91109

DAVID L. JAUNCEY
Division of Radiophysics, CSIRO, Epping, NSW 2121, Australia

DAVID L. MEIER
Jet Propulsion Laboratory, California Institute of Technology, Pasadena, California 91109

ANASTASIOS K. TZIOUMIS
University of Sydney, Sydney, NSW 2006, Australia
and
Nuffield Radio Astronomy Laboratories, Jodrell Bank, Macclesfield, Cheshire SK11 9DL, United Kingdom

JON ABLES AND ROBERT BATCHELOR
Division of Radiophysics, CSIRO, Epping, NSW 2121, Australia

JOHN FAULKNER
Department of Astronomy, University of Southern California, Los Angeles, California 90007

JOHN GATES
Division of Radiophysics, CSIRO, Epping, NSW 2121, Australia

BEN GREENE
Division of National Mapping, Belconnen, ACT 2601, Australia

P. A. HAMILTON
University of Tasmania, Hobart, Tasmania 7001, Australia

BRUCE R. HARVEY
School of Surveying, University of New South Wales, Kensington, NSW 2033, Australia
and
Division of Radiophysics, CSIRO, Epping, NSW 2121, Australia

RAYMOND F. HAYNES
Division of Radiophysics, CSIRO, Epping, NSW 2121, Australia

BEN JOHNSON
Ford Aerospace and Communications Corporation, Sunnyvale, California 94088

KURT LAMBECK
Research School of Earth Sciences, Australian National University, Canberra, ACT 2601, Australia

ALAN P. LOUIE
Jet Propulsion Laboratory, California Institute of Technology, Pasadena, California 91109

PETER MCCULLOCH
University of Tasamania, Hobart, Tasmania 7001, Australia

GRAHAM MOOREY
Division of Radiophysics, CSIRO, Epping, NSW 2121, Australia

DAVID D. MORABITO
Jet Propulsion Laboratory, California Institute of Technology, Pasadena, California 91109

GEORGE D. NICOLSON
CSIR, National Institute for Telecommunications Research, Johannesburg, South Africa

ARTHUR E. NIELL
Jet Propulsion Laboratory, California Institute of Technology, Pasadena, California 91109
and
Haystack Observatory, NEROC, Westford, Massachusetts 01886

 0004-6256/89/010001-26$00.90

J. G. Robertson
University of Sydney, NSW 2006, Australia
and
Anglo-Australian Observatory, Epping, NSW 2121, Australia

Gregory R. Royle
University of Tasmania, Hobart, Tasmania 7001, Australia

Lyle Skjerve and Martin A. Slade
Jet Propulsion Laboratory, California Institute of Technology, Pasadena, California 91109

O. B. Slee
Division of Radiophysics, CSIRO, Epping, NSW 2121, Australia

Artur Stolz
School of Surveying, University of New South Wales, Kensington, NSW 2033, Australia

Arthur Watkinson
University of Sydney, Sydney, NSW 2006, Australia

Ann E. Wehrle
Jet Propulsion Laboratory and California Institute of Technology, Pasadena, California 91109
and
Department of Astronomy, University of California, Los Angeles, California 90024

Alan E. Wright
Division of Radiophysics, CSIRO, Epping, NSW 2121, Australia
Received 14 July 1988; revised 9 March 1989

ABSTRACT

Six radio telescopes were operated as the first southern hemisphere Very Long Baseline Interferometry (VLBI) array in April and May 1982. Observations were made at 2.3 and 8.4 GHz. This array provided VLBI modeling and hybrid imaging of celestial radio sources in the southern hemisphere, high-accuracy VLBI geodesy between southern hemisphere sites, and subarcsecond radio astrometry of celestial sources south of declination $-45°$. We discuss the goals and implementation of the array, explain the methods of modeling and hybrid image production, and summarize the VLBI structure of the sources that were observed. Details of the imaging results on three individual sources, as well as some of the astrometric results and related optical identification work, appear in separate papers in this issue. The geodetic results have been published elsewhere.

I. INTRODUCTION

With the advent of Very Long Baseline Interferometry (VLBI) in the late 1960s, astronomers began to study radio-source structural detail with an angular resolution finer than 0.001 arcsec, far surpassing the capabilities at other wavelengths. At the same time, VLBI was also developed as a tool for performing high-accuracy geodetic and astrometric measurements, with present accuracies reaching a few centimeters and a few milliarcseconds (mas), respectively. VLBI imaging requires measurements to be made simultaneously from several radio telescopes spread over a large geographical area. While networks of antennas have been organized in the northern hemisphere over the last decade, they have poor capability for mapping sources in the southern hemisphere, where the antennas have little common sky visibility. Previous VLBI observations using southern hemisphere antennas have provided an insufficient number of baselines for source imaging (Gubbay *et al.* 1972, 1977; Preston *et al.* 1983a,b). An array of southern antennas is necessary for such work. In addition, VLBI geodesy in the southern hemisphere and VLBI astrometry in the far south require VLBI-instrumented southern antennas.

This paper describes the implementation of a temporary six-antenna VLBI array in the southern hemisphere (Preston *et al.* 1984). The experiment was a cooperative effort of both astronomers and geodesists and was conceived and organized jointly over a 2 yr period by the Jet Propulsion Laboratory and the Division of Radiophysics of the Commonwealth Scientific and Industrial Research Organization (CSIRO) in Australia. In addition, other Australian research organizations, observatories, and universities, as well as the Hartebeesthoek Radio Astronomy Observatory in South Africa participated (see author list).

In addition to the array, we discuss the methods of model fitting and hybrid imaging that were employed, including the calibration procedure, and summarize the VLBI structure for the 29 observed objects. More detailed descriptions of three of the more interesting sources are presented separately in this issue: Centaurus A ($1322-427$) by Meier *et al.*(1989), Sagittarius A ($1742-289$) by Jauncey *et al.* (1989a), and $1934-638$ by Tzioumis *et al.* (1989). The astrometric results appear in Jauncey *et al.* (1989b) and Morabito *et al.* (1986). Jauncey *et al.* (1989b) also contains a comparison of optical and radio astrometric results. Related optical identification work resulting from the astrometric results also appears in this issue (Jauncey *et al.* 1989c). The geodetic results have been published separately by Stolz *et al.* (1983) and Harvey *et al.* (1983).

II. THE ARRAY

The experiment was named the Southern Hemisphere VLBI Experiment, or SHEVE. Observations were performed over a 2 week period between 0500 UT on 20 April 1982 and 2400 UT on 3 May 1982. The details of the six antennas involved in SHEVE are shown in Table I, and their locations are shown on the map in Fig. 1. Three of these sites—Tidbinbilla (NASA Deep Space Station 43), Parkes, and Fleurs—formed an approximately equilateral triangle with antenna separations of about 250 km. The two other Australian antennas, Hobart and Alice Springs, are separated from the small triangle by about 1000 and 2000 km, respectively. The sixth antenna, Hartebeesthoek, is located in South Africa about 9700 km from the small triangle.

All six of the antennas operated at 2.3 GHz, while two of the antennas, Tidbinbilla and Parkes, also observed some sources at 8.4 GHz. All sites recorded a 1.8 MHz bandwidth with right-circular polarization using a Mark II VLBI recording system (Clark 1973). Bandwidth-synthesis instrumentation was installed at Tidbinbilla, Parkes, and Fleurs, which allowed a pair of 2 MHz bands separated by 38 MHz to be sampled on alternate seconds. This provided the accurate measurements of the differential time of arrival of a signal at two antennas needed for high-precision geodesy and astrometry.

III. GOALS OF THE EXPERIMENT

a) Astrophysics

All six antennas participated in the fine-scale mapping of celestial radio sources. The data from the five Australian antennas were used to produce models and hybrid maps of sources with minimum fringe spacings of about 12 mas and an angular resolution of about 5 mas, an improvement of almost four orders of magnitude over previously existing southern hemisphere radio-mapping instruments. A plot of the Australian u,v coverage for the sources 0438 − 436 is shown in Fig. 2.

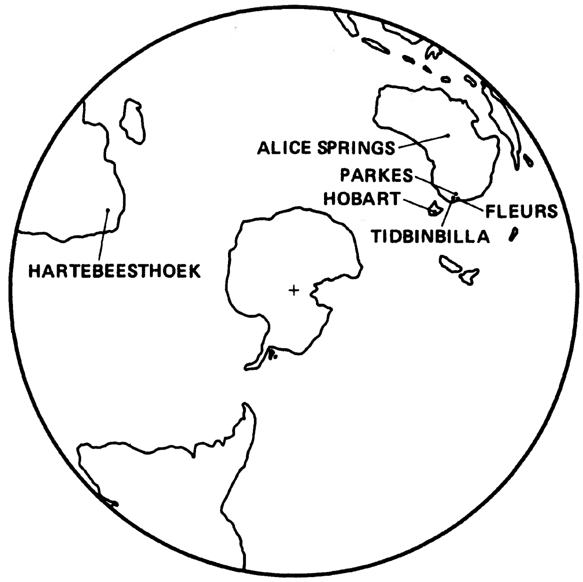

FIG. 1. Locations of SHEVE antennas.

The baselines from the five Australian antennas to the South African antenna yielded fringe spacing of about 3 mas. These baselines provided information on the extremely fine-scale structure of each source, but the data were not often included directly in the modeling and hybrid mapping of the sources due to the disparity in length between these baselines and those within Australia, as well as due to the limited u,v coverage obtained on the Hartebeesthoek baselines.

The compact structure of 29 southern hemisphere radio sources was investigated at 2.3 GHz. These sources included Centaurus A (the nearest active galaxy), the flaring binary star system Circinus X-1, the Vela pulsar, and the most distant known radio quasar (2000 − 330). In addition, Sagittarius A, the center of our galaxy, and Centaurus A were observed at 8.4 GHz on the Parkes–Tidbinbilla baseline. A list of the observed sources along with optical identifications and redshifts appears in Table II.

Each source was observed for periods totaling 3–15 hr, with the observing periods usually being shared with alter-

TABLE I. Details of SHEVE antennas.

Antenna name & abbreviation	Longitude (degrees °)	Latitude (degrees °)	Elevation (m)	Baseline[a] (km)	Size (m)	Frequency (GHz)	Receiver Type	$T_s(z)$ (K)	Mount	Frequency Standard
TIDBINBILLA (DS43)	-148.98	-35.22	656	...	64	2.29	TWM	17	ALTAZ	H-Maser
						8.42	TWM	25		
PARKES (PRKS)	-148.26	-32.82	392	274.75	64	2.29	FET	120	ALTAZ	H-Maser
						8.42	FET	140		
FLEURS (FLRS)	-150.76	-33.68	41	236.68	13.7	2.29	FET	230	EQUAT	Rubidium
HOBART[b] (HBRT)	-147.51	-42.65	50	835.29	13.7	2.29	FET	250	EQUAT	Rubidium
ALICE SPRINGS (ALSP)	-133.88	-23.61	200	1939.00	9.1	2.29	FET	230	ALTAZ	Rubidium
HARTEBEESTHOEK (HART)	-27.68	-25.89	1391	9589.24	26	2.29	TWM	35	EQUAT	Rubidium

[a]Baseline measured between each antenna and Tidbinbilla (DS43).
[b]A new 26 m antenna was erected at Hobart subsequent to SHEVE.

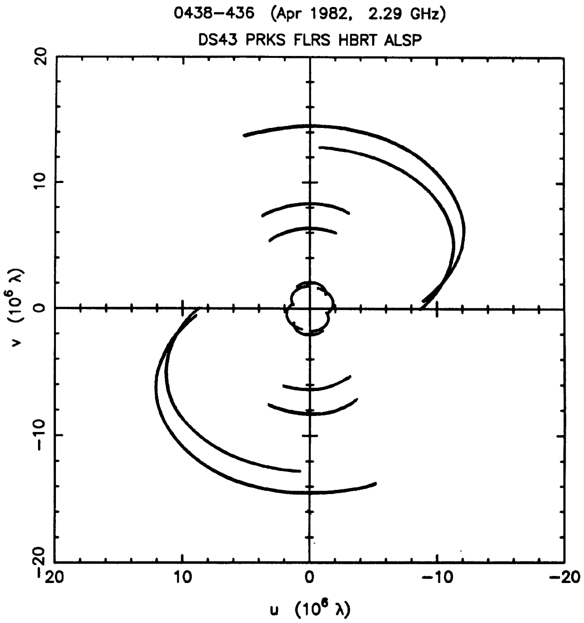

FIG. 2. Australian (u,v) coverage for 0438 − 436 at 2.29 GHz.

TABLE II. The SHEVE sample of 29 sources.

Source name	ID	z
0047-579	Quasar	1.797
0208-512	Quasar	1.003
0237-233	Quasar	2.223
0403-132	Quasar	0.571
0405-123	Quasar	0.574
0438-436	Quasar	2.852
0521-365	N Galaxy (BL Lac)	0.055
0537-441	Quasar	0.894
0637-752	Quasar	0.651
0743-673	Quasar	1.512
0833-450	The VELA pulsar.	
0834-201	Quasar	2.752
1104-445	Quasar	1.598
1215-457	Quasar	0.529
1322-427	Galaxy (NGC5128,Cen A)	0.002
1409-651	Sb Galaxy	0.0015
1421-490	Unidentified	
1424-418	Quasar	1.522
1516-569	Cir X-1, a flaring binary stellar system.	
1610-771	Quasar	1.710
1718-649	Spiral Galaxy	0.014
1742-289	Sag A, the galactic center.	
1921-293	Quasar	0.352
1934-638	Galaxy	0.183
2000-330	Quasar	3.780
2203-188	Quasar	0.618
2245-328	Quasar	2.268
2326-477	Quasar	1.299
2345-167	Quasar	0.576

nating observations of another source. The final schedule was a compromise between the need to produce a general idea of the angular structure of a large number of new (to VLBI) southern sources, and the desire to provide detailed maps of a small number of selected sources. Consequently, detailed maps are available for only three sources, while general models have been derived for a further 25. One source was not detected (1409 − 651).

Many other sources were observed at 2.3 GHz at only a single hour angle on the Tidbinbilla to Hartebeesthoek baseline. This provided survey information on milliarcsecond structure and was part of a full-sky VLBI survey (Preston *et al.* 1985).

b) Astrometry

Over the past 15 years astrometric observations with connected interferometers have provided radio-position catalogs with accuracies better than 0.1 arcsec, and VLB interferometers have reached accuracies approaching 0.001 arcsec. To date, such measurements have reached to about − 40° declination with northern hemisphere instruments.

Farther south, radio-position accuracies have been limited to about 1 arcsec. In order to extend higher-accuracy radio-astrometric catalogs to the far south, we used *S/X* band bandwidth-synthesis measurements on the Parkes–Tidbinbilla baseline to measure the positions of six radio sources south of − 45° declination. These were extragalactic sources chosen to span the sky in right ascension and to be strong, compact radio sources with bright optical counterparts. Positional accuracies were about 0.1 arcsec (Jauncey *et al.* 1989b), and were referenced to the existing VLBI source grid north of − 45° declination.

In addition, the VLBI data from the sources observed only between Parkes and Hartebeesthoek, as part of the all-sky VLBI survey program, yielded positional accuracies of typically 0.3 arcsec (Morabito *et al.* 1986). These positions, combined with earlier position determinations from the VLBI all-sky survey, allowed the optical identification of 158 compact radio sources, mostly from the southern hemisphere (Jauncey *et al.* 1989c). The optical identifications are mainly quasars, sources whose compact optical and radio structures provide ideal candidates for the unification of optical and radio celestial reference frames.

c) Geodesy

Only the five Australian antennas participated in the geodesy portion of SHEVE (Stolz *et al.* 1983; Harvey *et al.* 1983). Bandwidth-synthesis measurements at both 2.3 and 8.4 GHz on the Tidbinbilla/Parkes baseline yielded three-dimensional relative position measurements of about 7–15 cm accuracy. Bandwidth-synthesis measurements at 2.3 GHz on the Tidbinbilla/Fleurs and Parkes/Fleurs baselines provided 15–30 cm accuracy. Single-channel (i.e., 1.8 MHz bandwidth) 2.3 GHz observations on the Tidbinbilla/Hobart and Tidbinbilla/Alice Springs baselines gave 1–2 m accuracy.

IV. INSTRUMENTATION DETAILS

Major logistical and engineering efforts were required to establish the temporary SHEVE VLBI array for the 2 week observing period. Of the six antennas involved in SHEVE, two had never been used for radio astronomy before (Alice Springs and Hobart), three had not been previously involved in VLBI experiments (Alice Springs, Fleurs,and Hobart), and another had no permanent VLBI instrumentation (Parkes), three needed improvement to the pointing system (Fleurs, Alice Springs, and Hobart), two required the installation of an S band receiver system (Fleurs and Hobart), and another the installation of an S/X receiver system (Parkes), and one required the transport of a hydrogen-maser frequency standard from the U. S. (Parkes). Time synchronization in Australia was done prior to the experiment by taking a transportable rubidium clock to each antenna. Also prior to the experiment, short observations of 3C 273 were made between Tidbinbilla and each of the antennas, and then correlated to confirm configuration and clock synchronization.

A significant engineering effort was required at each of the three smaller Australian antennas as described below:

At Hobart, site preparation commenced with the felling of trees to clear the antenna horizon. A minicomputer was purchased and programmed to provide antenna pointing/slewing control, and pre-experiment measurements were made to determine antenna performance. The Hobart antenna allowed only limited hour-angle coverage in the far south. During the course of the experiment large offsets in antenna pointing occasionally appeared.

The antenna at Alice Springs is part of the Australian Landsat Facility and is instrumented at 2.3 GHz, so the existing feed and front end were utilized for the VLBI experiment. VLBI was run on a "noninterference basis" with the observing spread around the station's Landsat commitments; usually 20–22 hr per day were available for VLBI. The Landsat antenna operates in an "auto-track" mode only, so it was necessary to provide the capability to drive the az–el antenna in celestial coordinates. This was accomplished by means of an external microprocessor that calculated source elevation and azimuth, which were then buffered into the Landsat control unit. At rf, a coaxial switch in the antenna pedestal accomplished the transfer from Landsat to VLBI operations.

Only one (X_3) of the six 13.7 m telescopes of the Fleurs Synthesis Telescope was used for SHEVE. These antennas are normally used at 1.4 GHz but were found to perform adequately at 2.3 GHz, and feed and receiver systems were installed. A major hardware and software effort was undertaken to provide full computer control of the antenna (Tzioumis 1985).

V. CALIBRATION AND ANALYSIS OF IMAGING DATA

a) Correlation, Coherence, and Noise

The imaging data were correlated on the Caltech/JPL five-station Mark II processor in Pasadena, California. Coherent integration time at 2.3 GHz was restricted to 2 min by a poor rubidium-frequency-standard performance at Alice Springs, causing a maximum loss in fringe amplitude of 5% for baselines to Alice Springs and 2% or less for the other baselines. All sources except 3C 273 were too weak to produce detectable fringes between two of the smaller antennas (Alice Springs, Fleurs, Hobart). As a result, the number of closure phases and amplitudes available for hybrid mapping (Readhead and Wilkinson 1978) was limited. In principle, it would have been possible to detect fringes on the weaker baselines for many sources using the "global fringe fitting" technique (Schwab and Cotton 1983), but this technique would have been extremely time-consuming with such a large dataset and therefore was not used. The minimum detectable correlation coefficient from our data is $3(\pm 1)\times 10^{-4}$, which agrees well with the expected value.

Bad data points were eliminated in the following way. Our procedure was to delete all points outside the range $\bar{\rho} - 2\epsilon < \rho < \bar{\rho} + 5\epsilon$, where ρ is the correlated amplitude of a given data point, $\bar{\rho}$ is the correlated amplitude averaged over a 10 min period, and ϵ is the size of the error bars on the data. The lower limit is more stringent since low points are more common, especially on the Alice Springs baselines, due to transitory coherence losses. Not culling these points would have biased the results.

b) A Priori Calibration

The correlation coefficients on each baseline were converted to correlated flux densities using the procedure described by Cohen *et al.* (1975). For the multiplicative scaling factor b which appears in this process, the usual Caltech value of $b = 1.239$ was used. Antenna efficiencies and gain curves were obtained for each antenna that had not been previously calibrated. System temperatures were monitored periodically during the experiment period.

c) Relative Calibration between Baselines

Among the 29 sources observed in SHEVE, three sources ($0537-441$, $1921-293$, and $2326-477$) appear essentially unresolved at 2.3 GHz on all Australian baselines and three more ($0208-512$, $0237-233$, and $2345-167$) were unresolved on the "inner triangle" baselines (Tidbinbilla–Parkes–Fleurs). These were used to calibrate the experiment so that the data were internally consistent, yielding relative 2.3 GHz calibrations between the Australian antennas with formal errors smaller than 3%. Our method for 2.3 GHz calibration is described below.

Tidbinbilla was used as our reference telescope, and we compared the correlated flux-density amplitudes on the different baselines. For an unresolved source, all baseline amplitudes must be equal. By computing the ratios of the amplitudes on two baselines involving a common antenna, we obtained relative gain corrections between the two other antennas. Then, by forming suitable products of these corrections, all antennas (except Hartebeesthoek) could be scaled to Tidbinbilla. Factors were computed for all dates in the 2 week SHEVE observation period when an unresolved or barely resolved source was observed to check for any variation on the different dates. Fleurs had pointing-offset problems on 29–30 April and its calibration factor had to be varied on those days. Both Fleurs and Hobart had intermittent pointing-offset problems throughout the experiment and the data needed to be treated with some caution. For the Hartebeesthoek antenna, we had to rely on *a priori* calibration because we could not be certain any sources were unresolved on such long baselines.

The observations of the Vela pulsar were excluded from the above analysis specifically to provide an independent check on the relative calibration. Although weak, the pulsar appeared as an unresolved 0.4 Jy source on each of the Tidbinbilla baselines within Australia, providing overall confirmation of the above calibration at the 5% level. Unfortunately, the pulsar was not observed at Hartebeesthoek.

The Australian data have no (u,v) crossings but a few near crossings confirmed our relative calibrations to within 10%.

d) Calibration of the Reference Antenna

To calibrate Tidbinbilla at 2.3 GHz, the following procedure was used. The maximum correlated flux density for each unresolved or barely resolved source obtained on our shortest and best signal-to-noise baseline, Tidbinbilla to Parkes, was compared with the total flux densities determined by an ongoing flux-monitoring project at Hartebeesthoek (unpublished results of G. D. Nicolson) and by total flux densities measured at Tidbinbilla during the experiment. This resulted in a multiplicative flux-density correction of 0.9 being applied to the correlated flux densities of the internally calibrated Australian array. The resulting overall correlated flux-density scale for the Australian array is accurate to about 10%, although the relative calibration errors assumed are less than 3%. The *a priori* calibration of Hartebeesthoek was also assumed to be accurate to 10%.

e) The Fitting of Gaussian-Component Models to the Data

As discussed earlier, most observations were fitted to models rather than hybrid mapped. In order to determine the structural information available in the data, source models involving elliptical Gaussian components were fitted to the closure phase and calibrated fringe amplitude data. As the baselines to Hartebeesthoek were considerably longer than any Australian ones, the former were often treated separately and not included in the model-fitting procedure with the Australian baselines.

Several steps were taken to restrict the number of free parameters in the models, so as to produce the simplest model consistent with the data:

(1) Models with the fewest free parameters were tried first and new free parameters were added only when the data clearly called for them.

(2) When possible, the data were fitted to circular rather than elongated components, reducing the nuber of parameters by two per component;

(3) If a position angle was indicated by the data, all components were initially assumed to lie on that position angle, unless there was strong evidence to the contrary.

All sources were initially fitted to single-component circular Gaussians and then to single-component elliptical Gaussians before proceeding further. Sources with beating in the correlated flux-density amplitudes on one or more baselines were then fitted first to double point sources and then to double circular Gaussians, if a drop in correlated flux from shorter to longer baselines indicated that one or more components were resolved. For sources with no obvious beating, the longer baselines were fitted first and additional concentric components were added only if the data required such. In most cases, a maximum of two components were required and in no case was more than one component allowed to be elongated unless both were concentric. Since the longer Australian baselines only provided sensitivity for the position-angle range of 20°–130°, our ability to detect source extensions is limited mainly to this region. Generally, in cases that required an elongated component, we found that the flux density of that component and its width were not independent. In such cases we fixed the width of all elongated components to zero (i.e., unresolved), yielding only a minimum flux density of such components, as the component might be partly resolved along its width.

In order to keep the more sensitive baselines from totally dominating the model, we artificially increased the error bars on the baselines from Tidbinbilla to Parkes and Fleurs so that they were equal to those of the Parkes–Fleurs baseline. This made the analysis less sensitive to any uncorrected systematic calibration errors.

As a result of this model-fitting procedure, we believe we have determined the simplest structure consistent with the VLBI observations. The actual sources are likely to be more complicated when observed with better (u,v) coverage, but they are not likely to be any simpler. In the next section we give a brief encyclopedic description of each source, discussing previously known properties, the results from model fitting, and hybrid mapping using the SHEVE data.

For 25 of the observed sources, these models were the final product of the imaging data. Three of the sources were hybrid mapped, with the models serving as starting points for the mapping procedure. The sources were: 0237 − 233, 0438 − 436, and 1934 − 638.

Of the 29 sources, three are discussed in detail in companion papers (Centaurus A by Meier *et al.* 1989; Sagittarius A by Jauncey *et al.* 1989a; and 1934 − 638 by Tzioumis *et al.* 1989). Brief individual source descriptions of all sources are presented in this paper.

VI. DESCRIPTIONS OF SOURCE MODELS

In the description of the SHEVE sources below, the optical identifications, magnitudes, and redshifts were taken from the compilation of data in the VLBI survey by Preston *et al.* (1985) and from Tzioumis (1987). The radio flux density at the SHEVE epoch and variability information, when available, were taken mainly from the 2.3 GHz total flux-density monitoring survey of Nicolson (unpublished) and occasionally from SHEVE total flux-density measurements. VLA results (resolution $< \sim 1''$) are taken from Ulvestad *et al.* (1981) and Perley (1982) unless otherwise noted. For the sake of brevity, the specific literature references for these earlier data are generally not given in the following source list, but can be recovered from the above papers. Models of the sources from the SHEVE data are based only on 2.3 GHz data from the Australian antennas unless otherwise noted, with angular resolution being about 5 mas. The data on Hartebeesthoek baselines are generally sparse and were only used to provide milliarcsecond detail to the larger structure with Australian baselines, generally by adding size or unresolved cores to components. The VLBI data and the best-fit models to these data are plotted in Fig. 3. Images formed from the best-fit models are shown in Fig. 4.

The individual sources are discussed below in right ascension order:

0047 − 579. An 18.5 mag quasar; $z = 1.797$; 2.3 GHz total flux density was 2.1 Jy and is 20% variable on a timescale of 2 yr. The source is adequately fitted with two concentric elongated components oriented with their major axes along a position angle 111° east from north. One component is 4 mas long with a strength of 1.2 Jy, while the other is 100 mas long with a strength of 0.34 Jy. Independent solutions using data from only the small Tidbinbilla–Parkes–Fleurs triangle or only the long Australian baselines to Alice Springs produce the same position angle for each component within 5°. The baselines to Hartebeesthoek indicate that the milliarcsecond nuclear structure is more complex than a single symmetric component and has a minimum flux density of 0.6 Jy.

0208 − 512. A 16.9 mag quasar; $z = 1.003$; 2.3 GHz total flux density was 4.3 Jy and had increased by 70% during the 4 yr preceding SHEVE. The Australian SHEVE data are

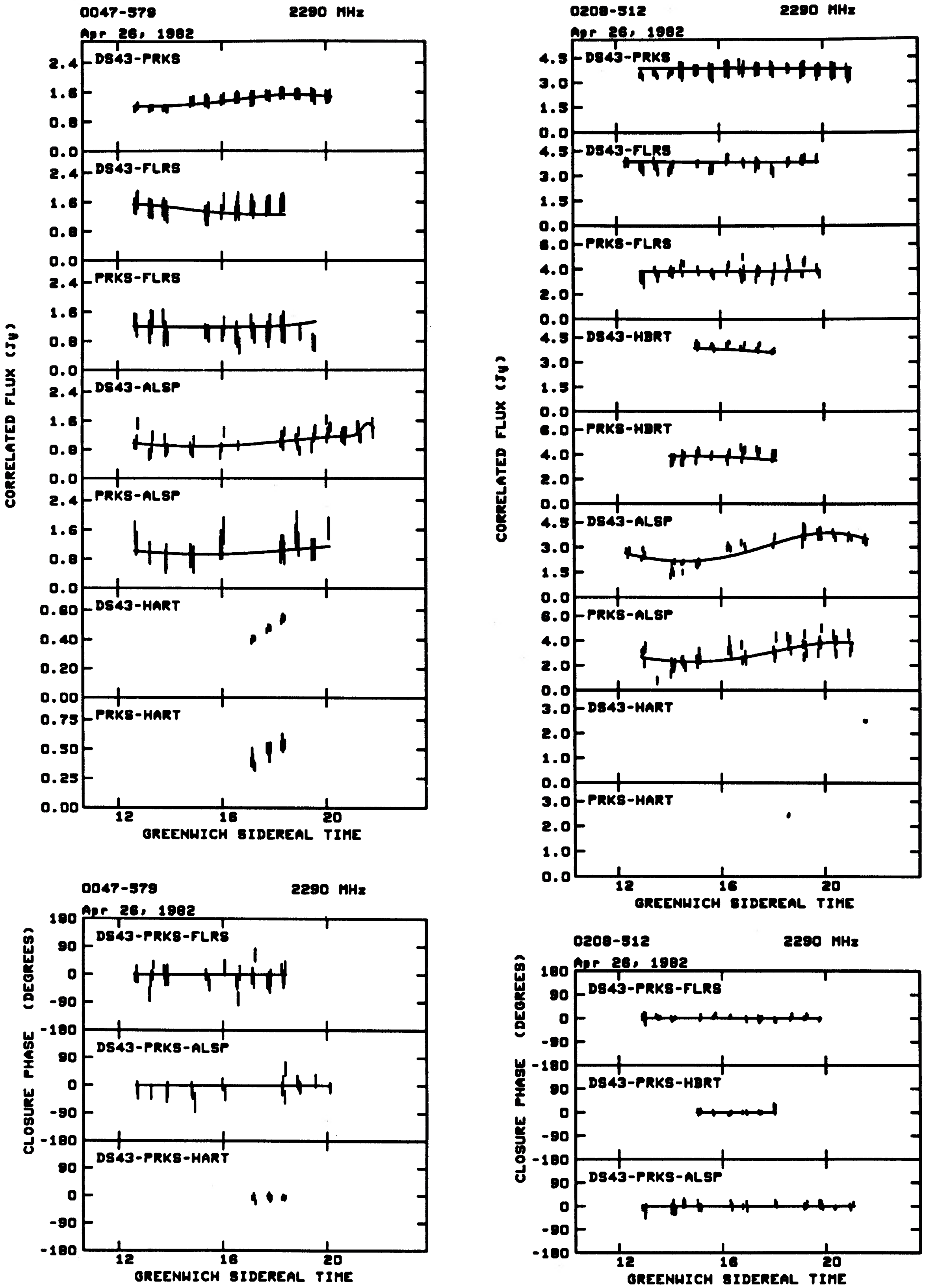

FIG. 3. Correlated flux densities and associated error bars for each source. Solid lines represent best-fit models.

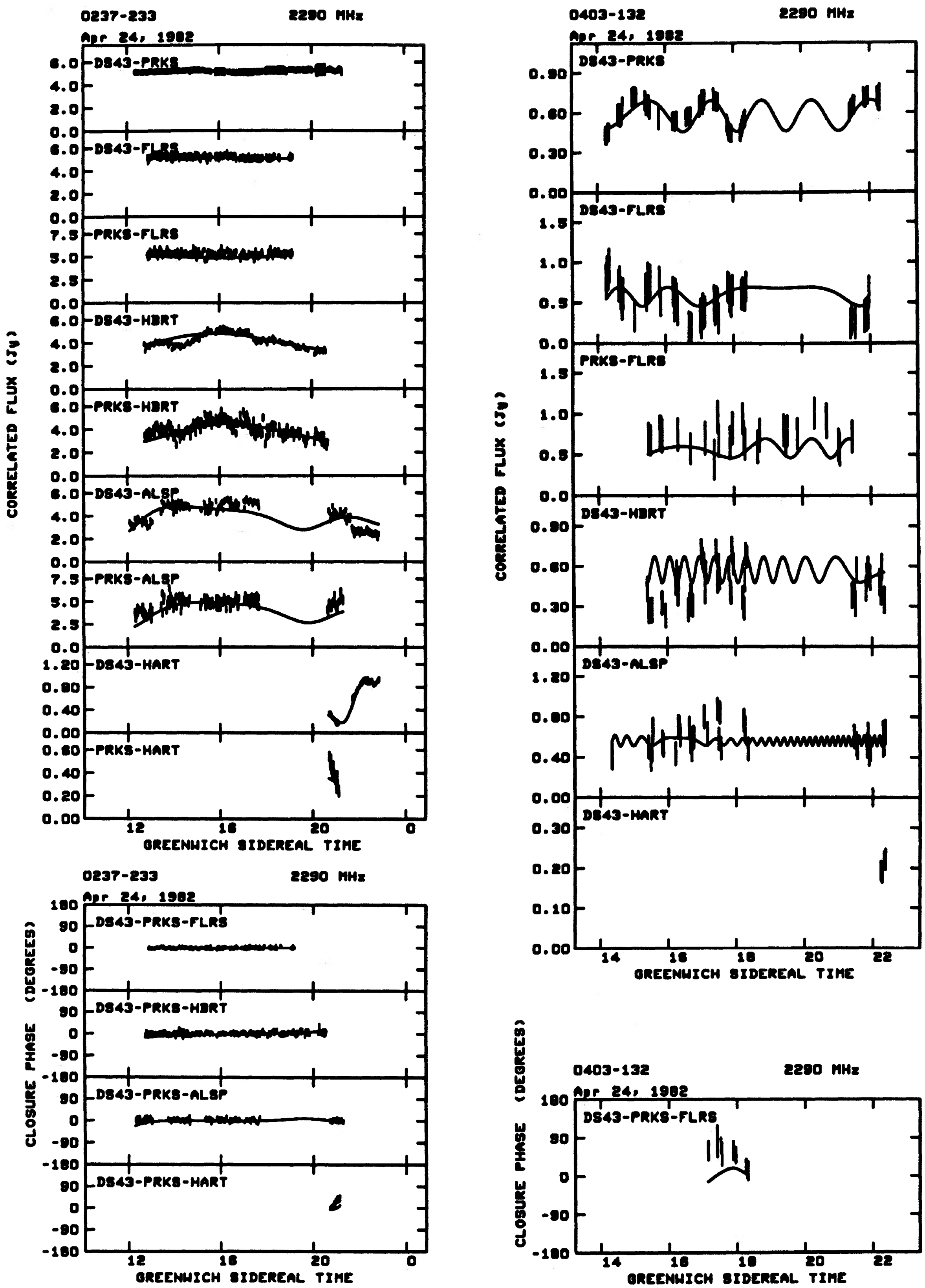

FIG. 3. (continued)

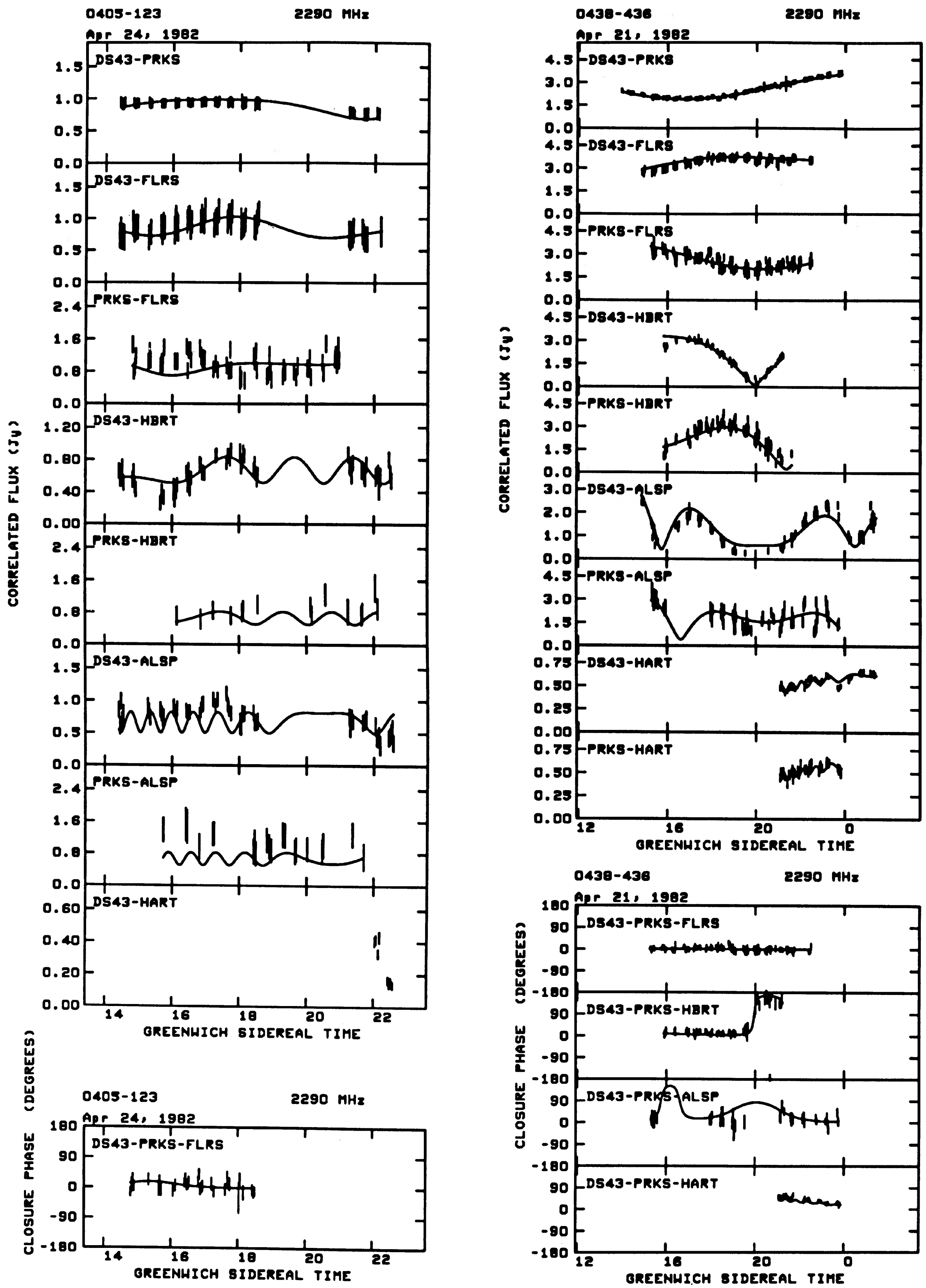

FIG. 3. (continued)

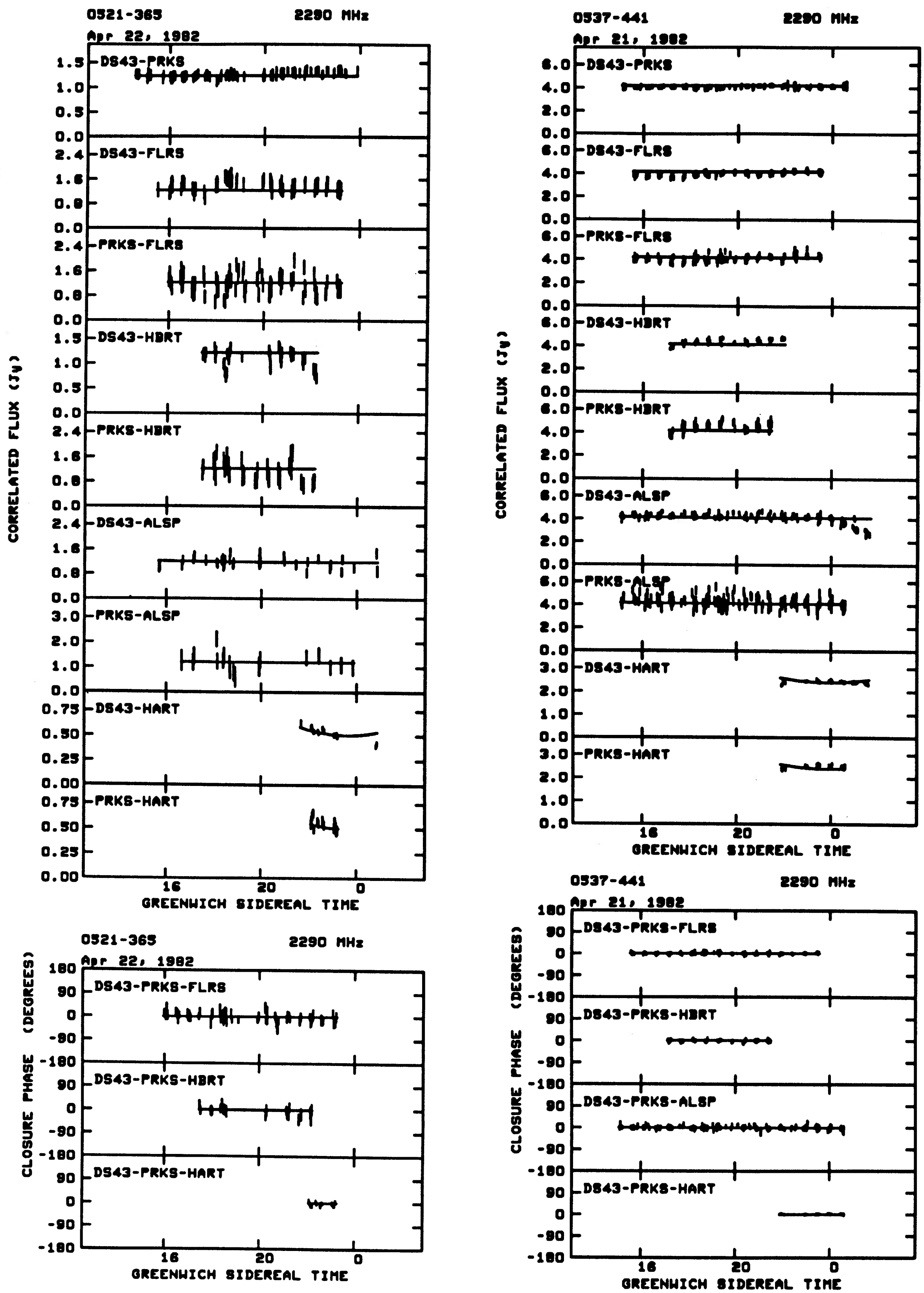

FIG. 3. (continued)

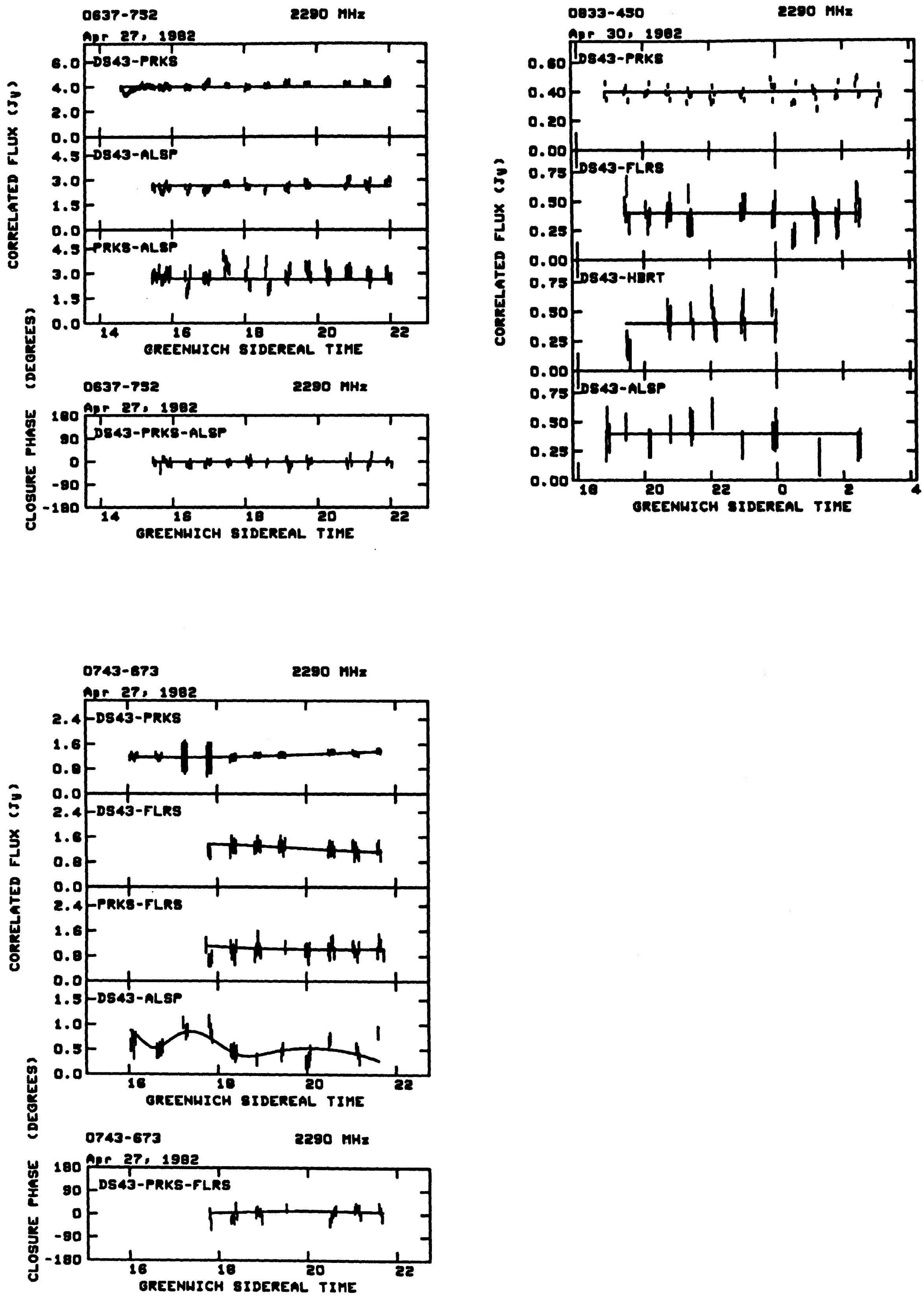

FIG. 3. (continued)

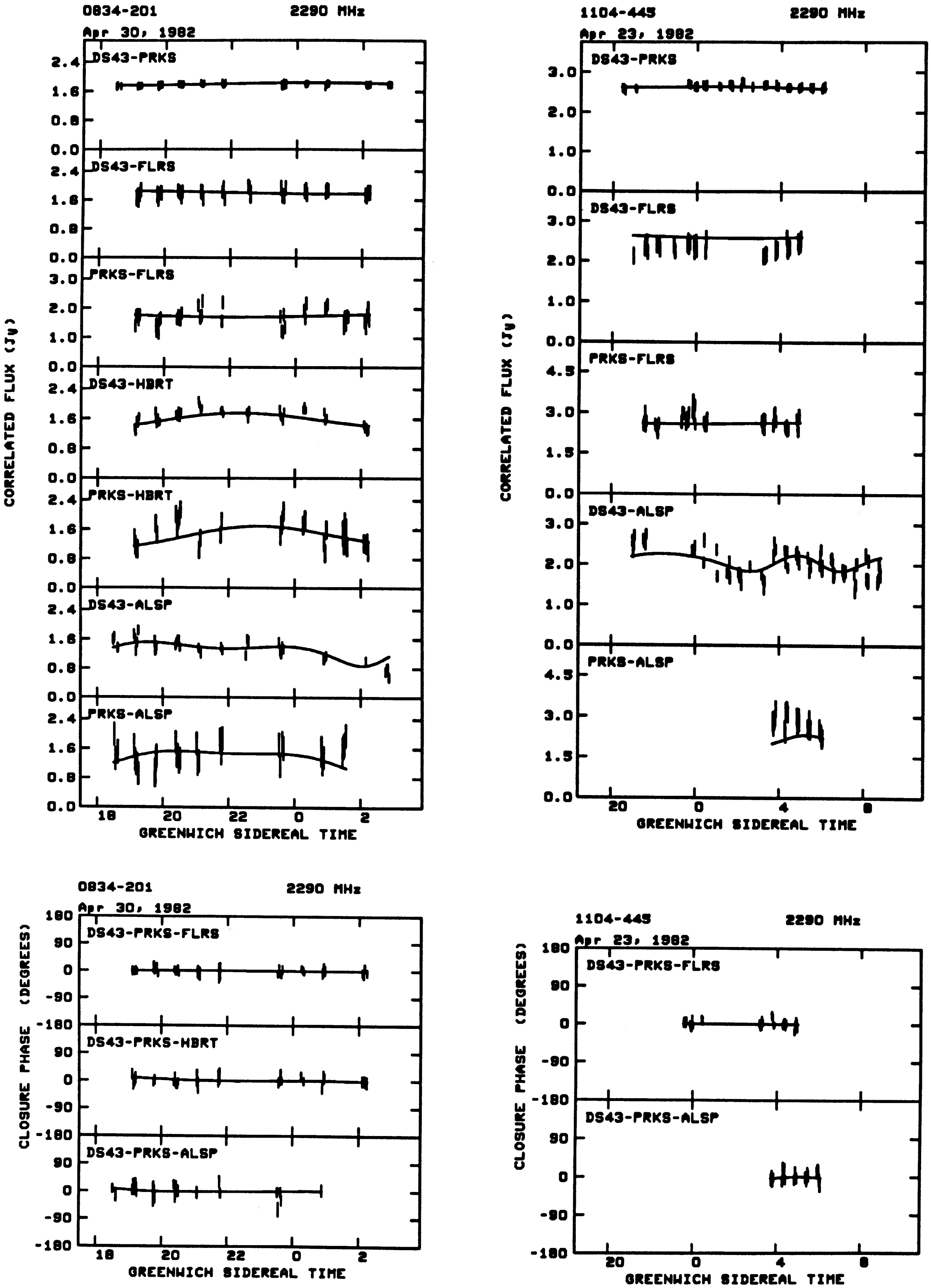

FIG. 3. (continued)

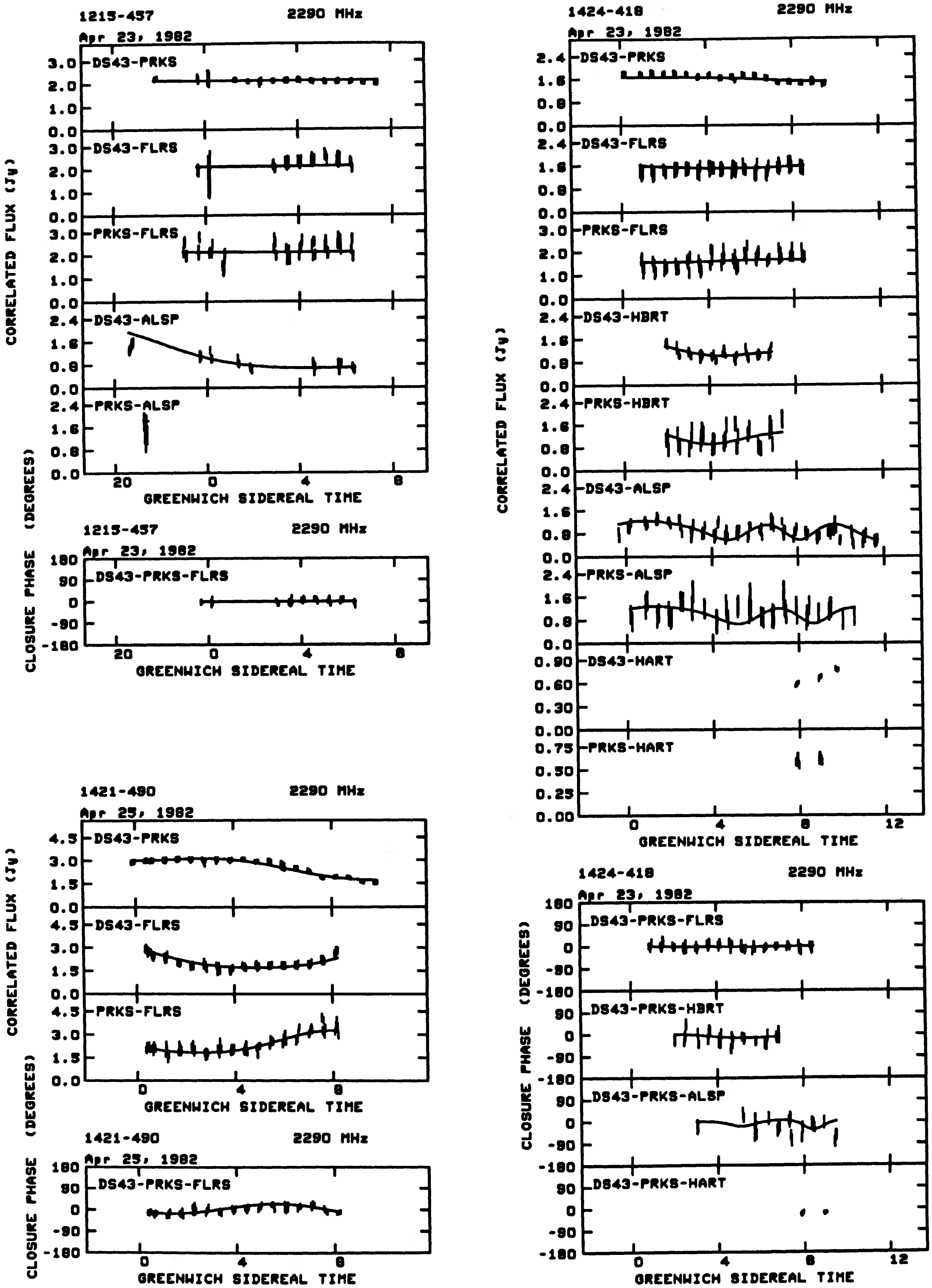

FIG. 3. (continued)

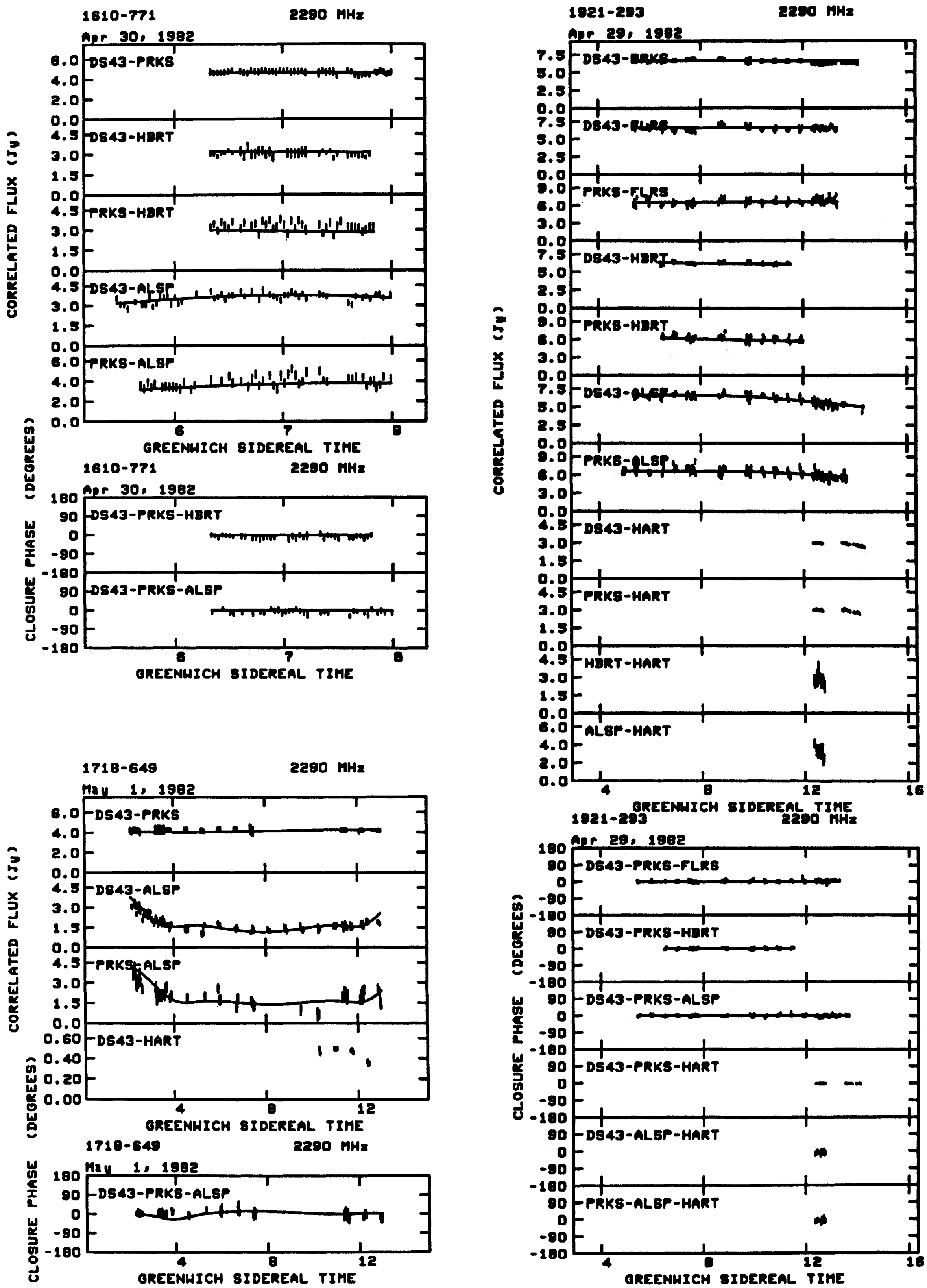

FIG. 3. (continued)

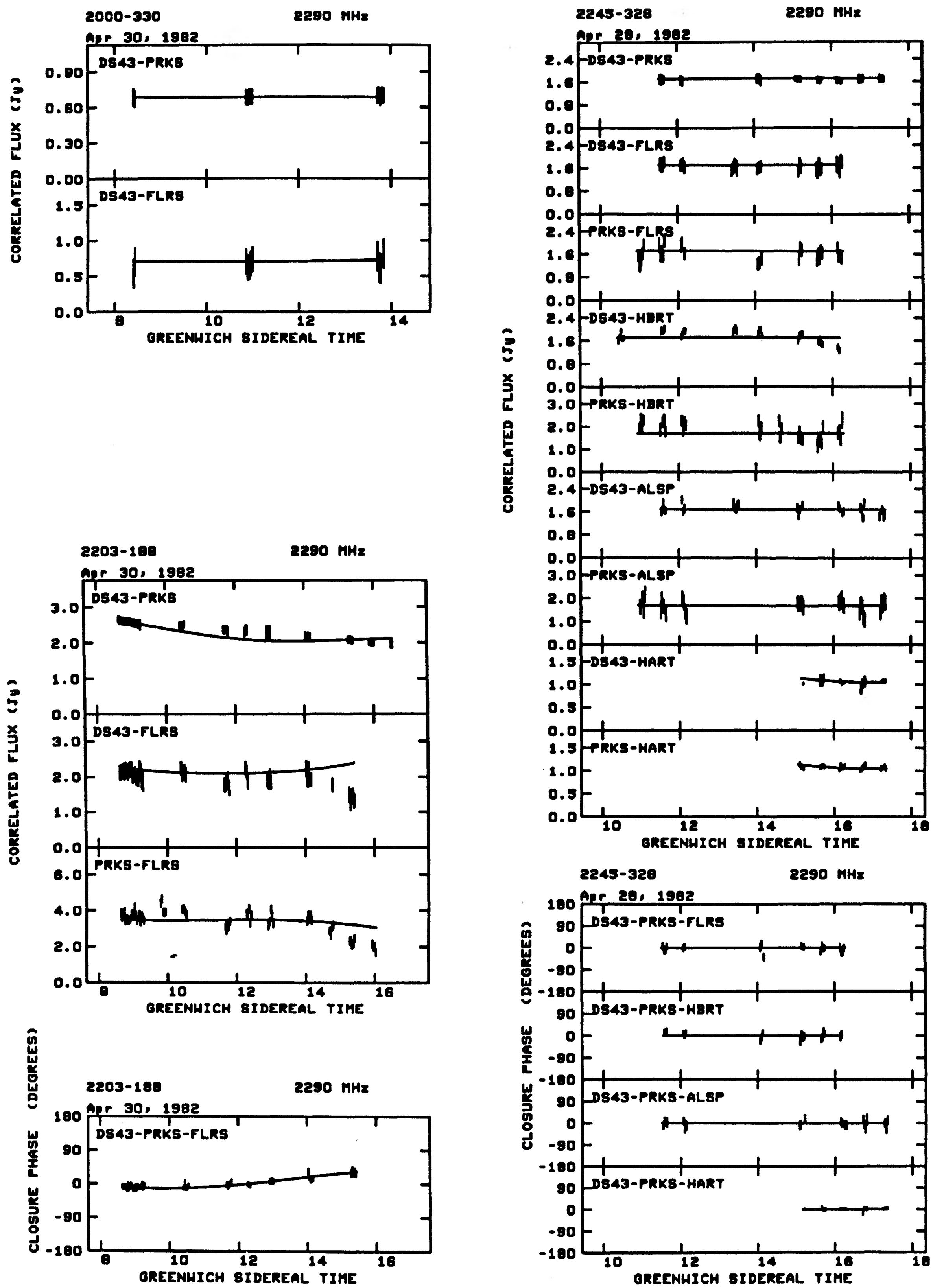

FIG. 3. (continued)

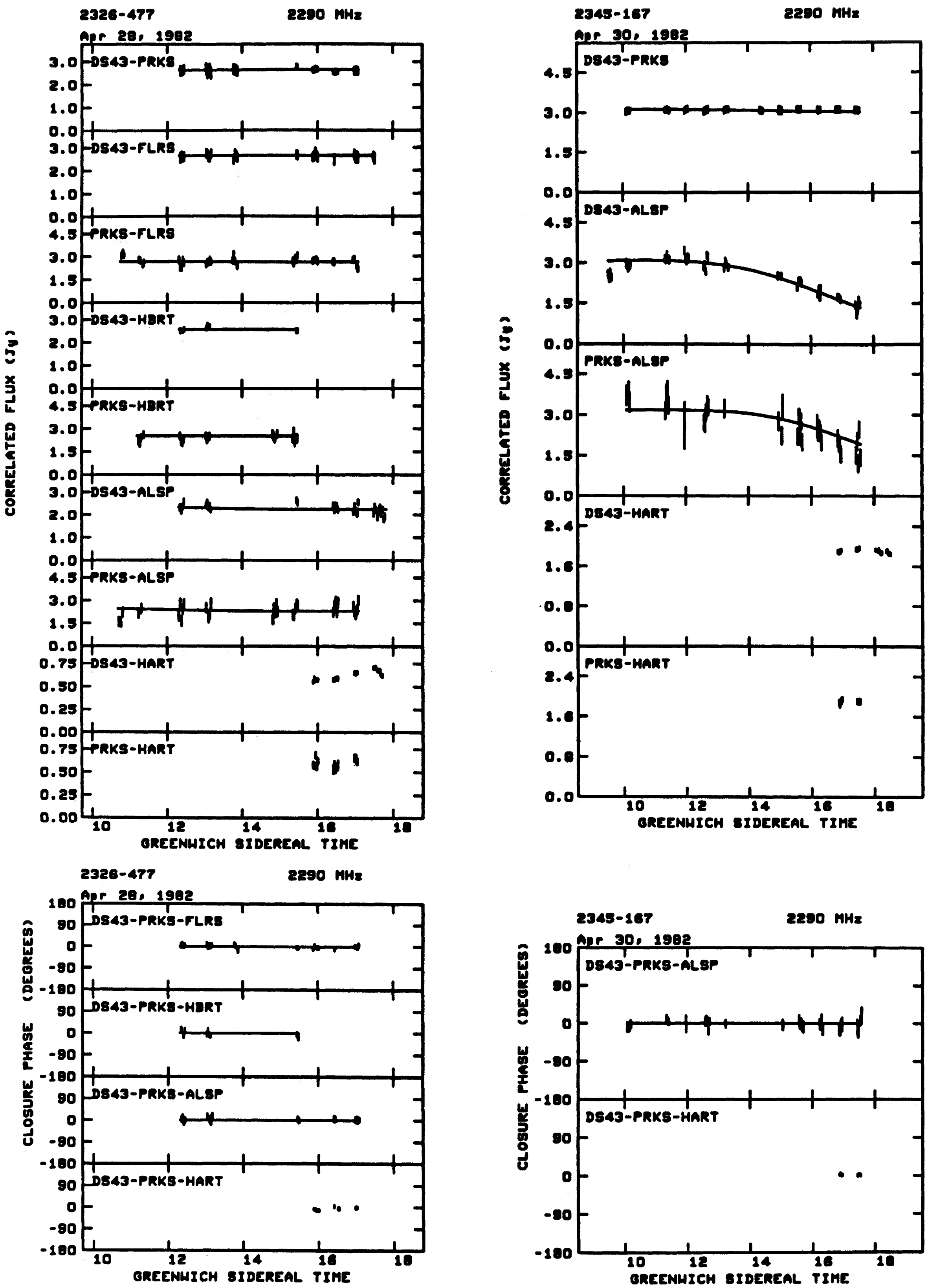

FIG. 3. (continued)

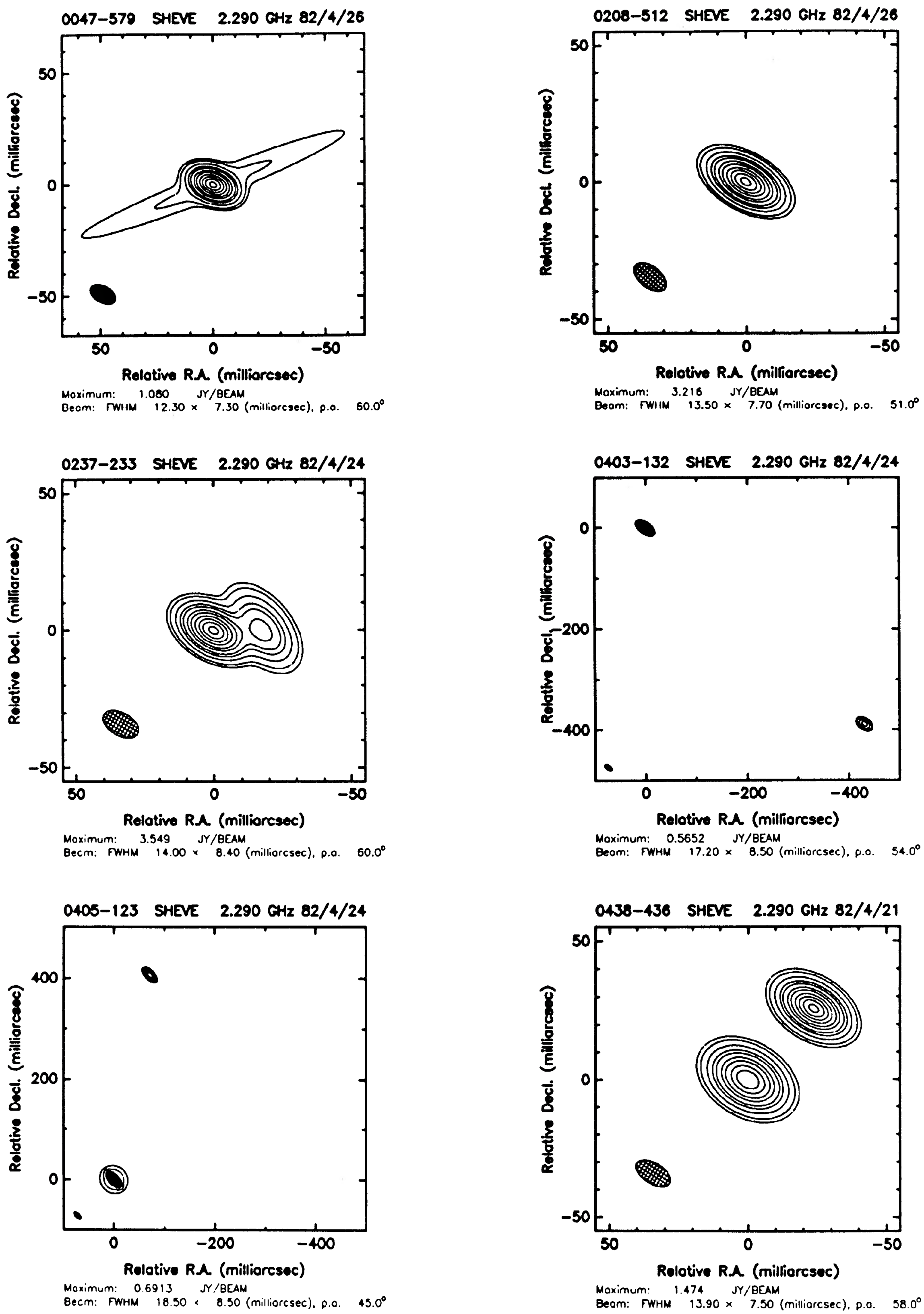

FIG. 4. VLBI images of SHEVE sources formed from source models. The images have been made by convolving the source models with the appropriate restoring beam (positive lobe of antenna pattern). The beams are shown crosshatched. Contour levels are at − 1%, 1%, 2%, 5%, 10%, 15%, 25%, 35%, 50%, 65%, 80%, and 95% of peak value.

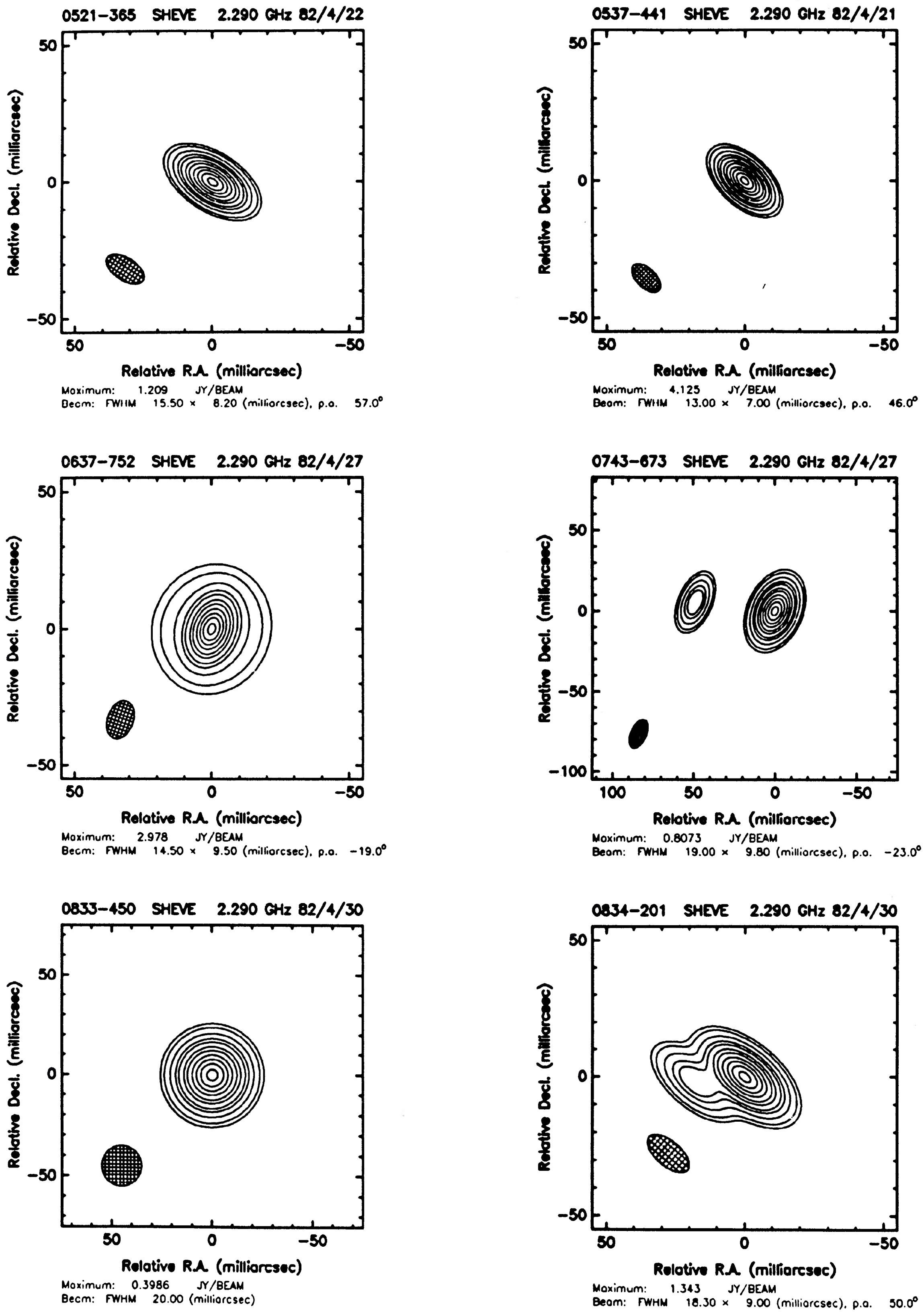

FIG. 4. (continued)

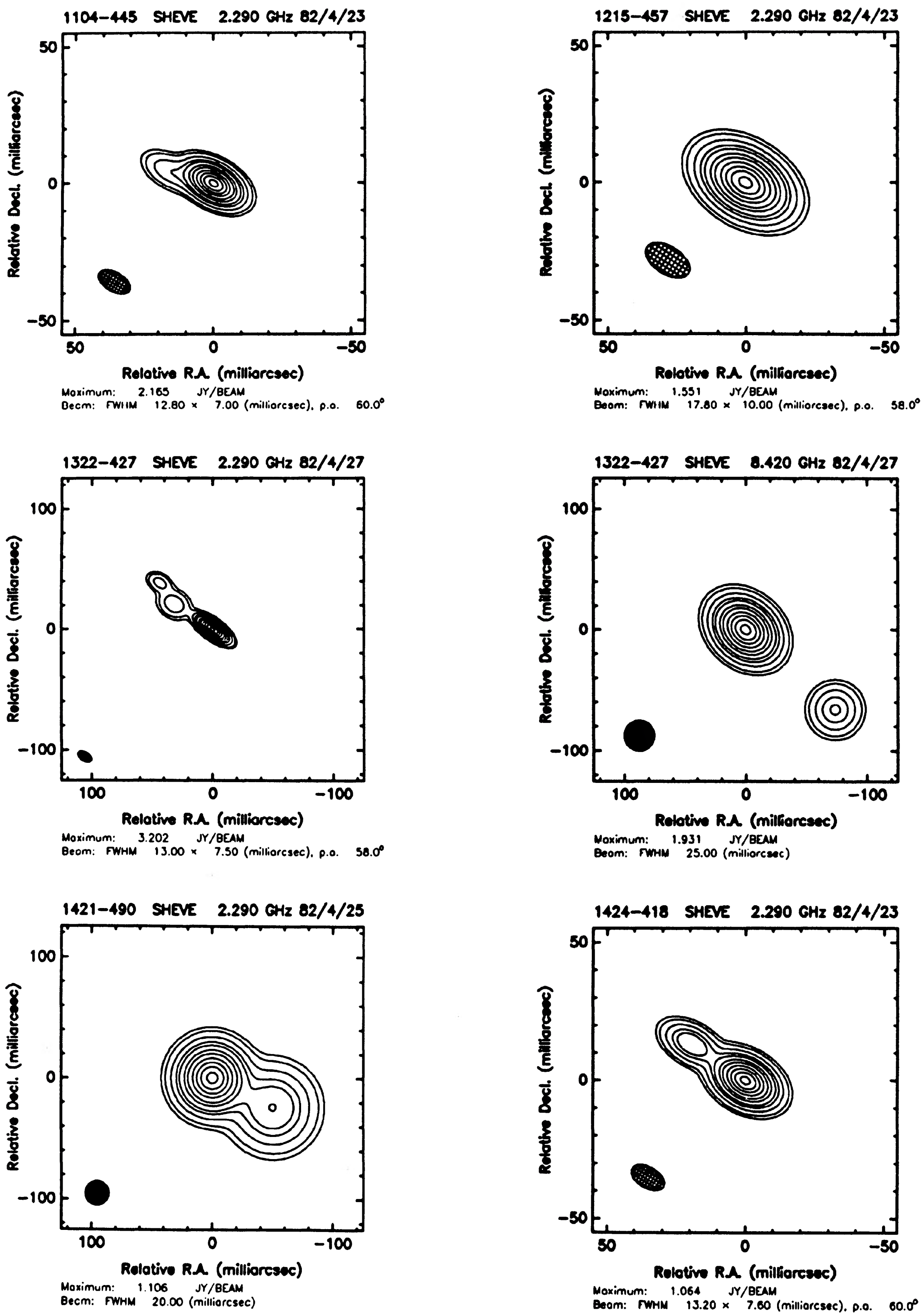

FIG. 4. (continued)

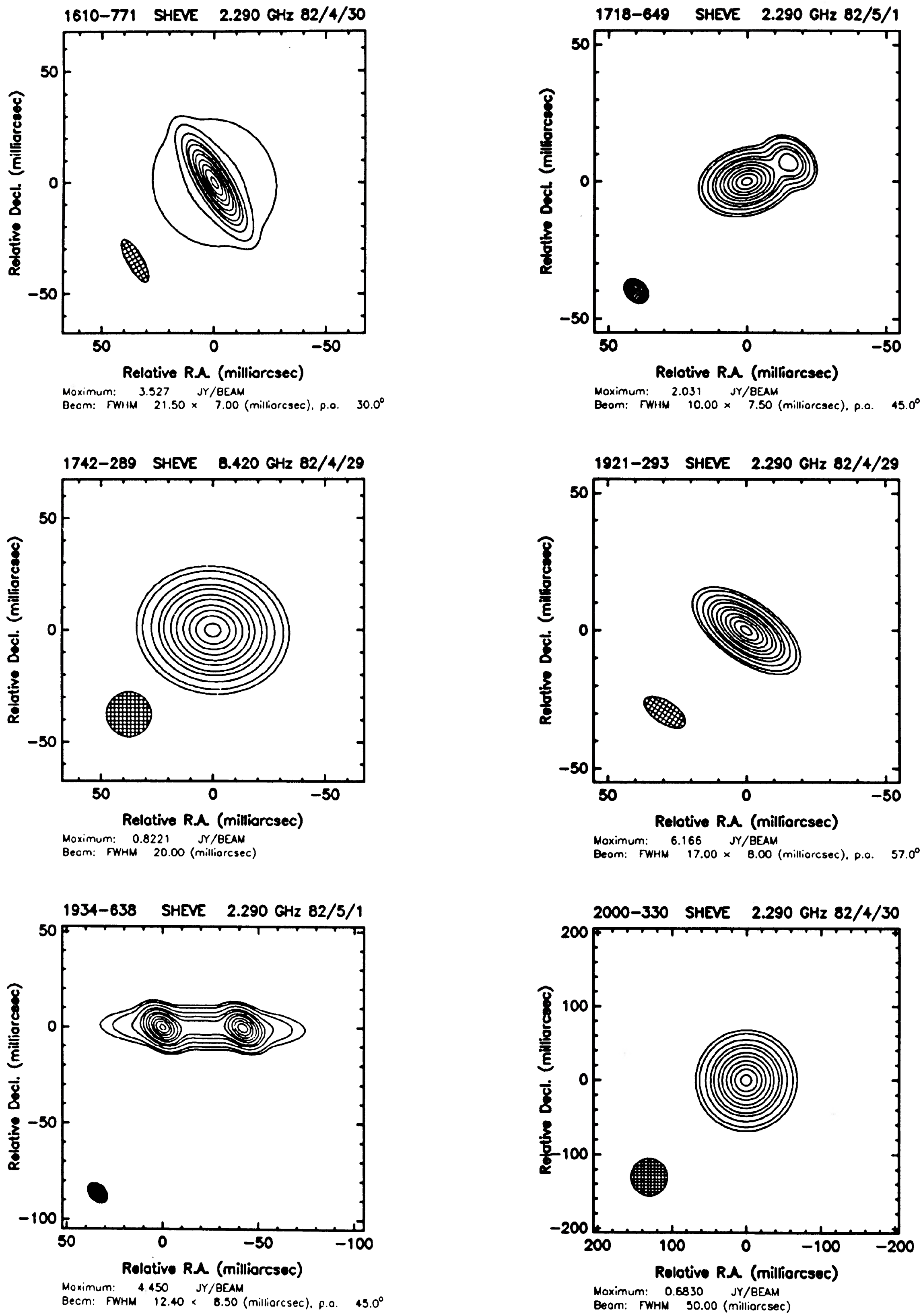

FIG. 4. (continued)

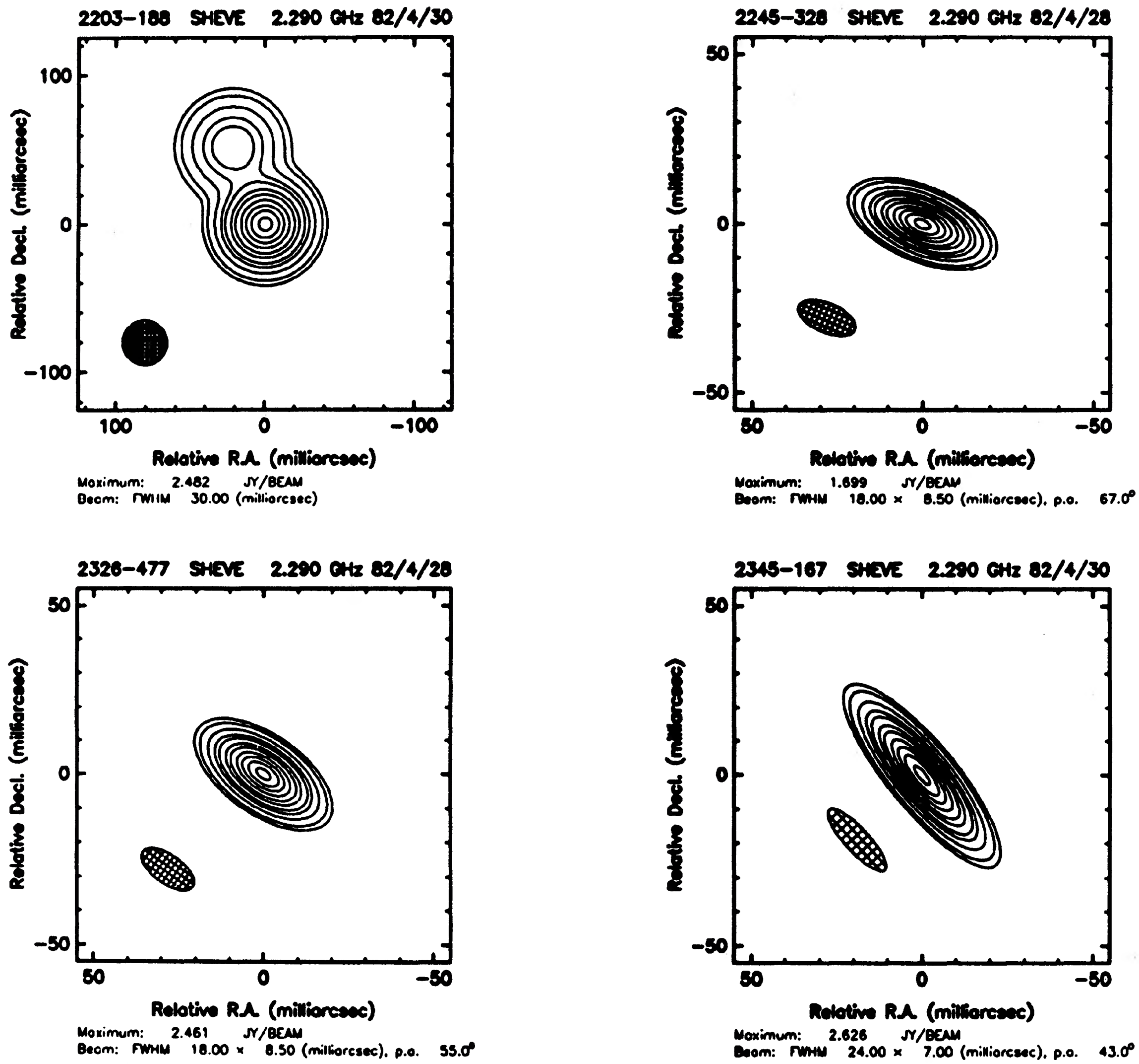

FIG. 4. (continued)

adequately represented by a 3.9 Jy source 7.7 mas long at position angle 78°. The baselines to Hartebeesthoek indicate the nuclear milliarcsecond structure has a minimum flux density of 2.5 Jy.

0237−233. A 16.6 mag quasar; $z = 2.223$; 2.3 GHz total flux density was 5.8 Jy with possible 10% variability on a timescale of 1 yr; unresolved with the VLA at 6 and 20 cm. The Australian SHEVE data show complex structure. A reasonable fit is obtained with two unequal point sources of 3.8 and 1.1 Jy, respectively, separated by 18 mas along a position angle of about 90°. There is not much information on which side the stronger component lies. There is some evidence for a third weak 0.3 Jy component roughly 56 mas away from the stronger component along the same position angle but no information on which side. A complete solution including the Hartebeesthoek baseline can be obtained by elongating the weaker component to 12 mas at a position angle of 20° and adding a 0.25 Jy core to it (model shown in Fig. 4). The stronger component is about 2.6 mas in size. A hybrid map of this source using only the Australian baselines is shown in Fig. 5.

0403−132. A 17.1 mag quasar (or "blazar;" Antonucci and Ulvestad 1984); $z = 0.571$; 2.3 GHz total flux denisty was 3.7 Jy with 10% variability over a 2 yr timescale; VLA indicates a core–jet structure for this source at 20 cm pointing toward the northeast with a position angle of 30° (Wardle, Moore, and Angel 1984). The Australian SHEVE data clearly show an unequal double source but so well resolved on even the shortest baselines that the position angle is difficult to determine. The best model yields a position angle of 48°, a separation of about 580 mas, and strengths of 0.58 and 0.12 Jy for the two unresolved components. The VLA and VLBI position angles are consistent to within 20°. The one baseline to Hartebeesthoek indicates a milliarcsecond core with a minimum flux density of 0.2 Jy.

0405−123. A 14.6 mag quasar; $z = 0.574$; 2.3 GHz total flux density was 2.4 Jy with 15% variability on 2 yr timescales. The Australian SHEVE data were fit by two point

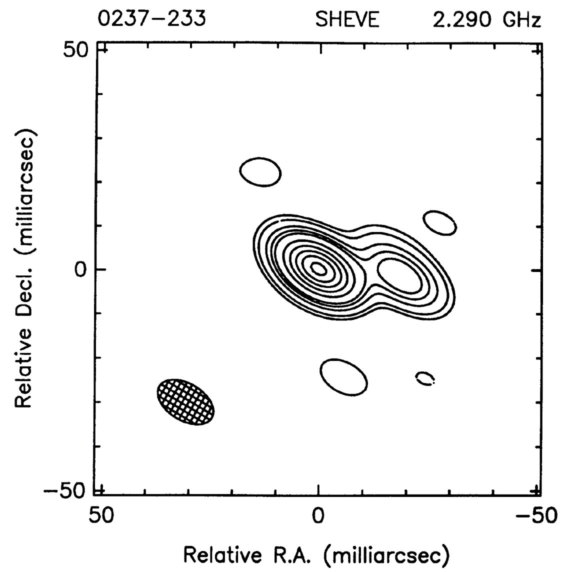

FIG. 5. Hybrid map of 0237 − 233 at 2.29 GHz. Contour levels are 3%, 5%, 10%, 15%, 20%, 35%, 50%, 65%, 80%, and 95% of peak.

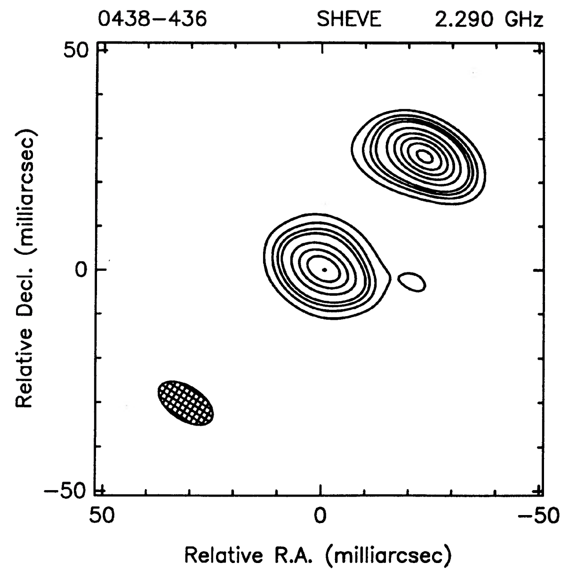

FIG. 6. Hybrid map of 0438 − 436 at 2.29 GHz. Contour levels are − 5%, 5%, 10%, 15%, 20%, 35%, 50%, 65%, 80%, and 95% of peak.

sources with a concentric circular Gaussian halo around one of them. The position angle is − 10° and the flux densities of the point source are 0.66 and 0.16 Jy. However, the separation of the sources is not well determined, but believed to be either 200 or 400 mas. The 400 mas model is shown in Fig. 4. The halo component has a diameter of 35 mas and a flux density of 0.27 Jy. The one baseline to Hartebeesthoek indicates that the nuclear milliarcsecond structure is more complex than a single symmetric component and has a minimum flux density of 0.4 Jy.

0438−436. An 18.8 mag quasar; $z = 2.852$; 2.3 GHz total flux density was 4.3 Jy and had dropped by a factor of 2 during the 12 yr preceding SHEVE. VLA maps at wavelengths of 6 and 20 cm (Perley 1985) show a 2 arcsec extension from the core at a position angle of about 10°. The large amount of Australian SHEVE data with good signal-to-noise are well fitted by two 1.9 Jy circular Gaussians separated by 35 mas at a position angle of − 43°. The southeast component appears to be slightly more extended than the northwest one (8 mas vs 5 mas). A large difference (53°) exists between VLA and VLBI position angle. A core–jet model for this source is physically more likely than a Phillip–Mutel double (Phillips and Mutel 1982) because of the high variability of the source. This is supported by the data on the baselines to Hartebeesthoek, which show one component to be much more resolved than the other. A complete model, which fits the data from the baselines to South Africa as well, can be obtained by adding a core source at the centroid of each component (model shown in Fig. 4). These cores have flux densities of 0.6 and 0.04 Jy with the stronger elongated along the position angle of 24° with a length of 1.3 mas. A hybrid map of this source using only Australian baselines is shown in Fig. 6.

0521−365. A 14.9 mag N galaxy whose nucleus is a BL Lac type object; $z = 0.055$; 2.3 GHz total flux density was 13.4 Jy. A VLA map at 2 cm shows a jet extending 6″ to the northwest from the nucleus at a position angle of − 55°, with a transversely extended knot 2″ into the jet and an opposing hotspot 8″ to the southeast of the nucleus (Keel 1986). The optical image also shows jetlike structure extending to the northwest with similar length and position angle (Danziger *et al.* 1979; Danziger *et al.* 1985; Cayatte and Sol 1987). The positions of the optical galaxy (Wardle, Moore, and Angel 1984) and the VLBI nucleus (Morabito *et al.* 1986) are coincident with the northwest compact VLA component. While the radio source is strong, the VLBI core is weak. Our Australian data are sparse and are adequately fitted with a point source of 1.2 Jy. Inclusion of the Hartebeesthoek data shows that all of the SHEVE data are consistent with a circular Gaussian source, 1.4 mas in diameter (model shown in Fig. 4).

0537−441. A 16.5 mag quasar; $z = 0.894$; 2.3 GHz total flux density is extremely variable (by almost a factor of 2) on timescales of 1–2 yr and was 4.7 Jy during SHEVE near the peak of an outburst; the source recently turned into a BL Lac object (Cristiani 1985). A VLA map at 20 cm (Perley 1985) shows an extension leading 5 arcsec to the northwest. The SHEVE data (including the Hartebeesthoek baselines) are adequately fitted by a circular Gaussian with a flux density of 4.2 Jy and a diameter of 1.1 mas.

0637−752. A 15.8 mag quasar; $z = 0.651$; 2.3 GHz total flux density was 5.9 Jy. The Australian SHEVE data are limited and are well fitted by an unresolved core of 2.6 Jy and a concentric circular Gaussian halo with a flux density of 1.5 Jy and a diameter of > 20 mas. No data were obtained on the baselines to Hartebeesthoek, but 2 yr earlier Preston *et al.* (1985) observed a correlated flux density of 0.96 Jy at 2.3 GHz on the Tidbinbilla to Hartebeesthoek baseline.

0743−673. A 16.4 mag quasar; = 1.512; 2.3 GHz total flux density was 3.3 Jy. The Australian SHEVE data are well fitted by two point sources with flux densities of 1.2 Jy and 0.2 Jy at a position angle of about 84° and separated by 49 mas. No data were obtained on the baselines to Hartebeesthoek, but 2 yr earlier Preston *et al.* (1985) observed a correlated flux density of 0.53 Jy at 2.3 GHz on the Tidbinbilla to Hartebeesthoek baseline.

0833 − 450 (Vela pulsar). A pulsar in our galaxy associated with the Vela supernova remnant. The Australian SHEVE data can be fitted by a point source with an equivalent continuum flux density of 0.40 Jy. There were no data on the baselines to Hartebeesthoek.

0834 − 201. A 19.4 mag quasar; $z = 2.752$; 2.3 GHz total flux density dropped by 40% during the 7 yr preceding SHEVE to a level of 1.9 Jy. The source appears unresolved on the VLA at 2, 6, and 20 cm. Two models fit the Australian SHEVE data equally well. Both models have two components with flux densities of 1.5 and 0.3 Jy, with a separation of 17 mas, and a position angle of 95°. One model, which is the model plotted, consists of a weak unresolved point source and a strong circular Gaussian component. The other model consists of a strong point source and a weak offset line jet. There are no SHEVE data on the baselines to Hartebeesthoek, but observations at 2.3 GHz on a similar-length baseline 6 yr earlier failed to detect the source with a detection limit of 0.1 Jy (Preston *et al.* 1985).

1104 − 445. An 18.2 mag quasar; $z = 1.598$; 2.3 GHz total flux density was 3.2 Jy. The Gaussian size measured with the VLA at 20 cm is ~6 arcsec. The Australian SHEVE data were fitted by a nearly unresolved circular Gaussian with a flux density of 2.5 Jy and a 4 mas diameter. The beating on the Tidbinbilla to Alice Springs baseline suggests an additional weak point source with a flux density of 0.2 Jy, separated by 17 mas from the main component along a position angle of about 75°. No data were obtained on baselines to Hartebeesthoek during the multibaseline coverage of this source, but data taken a few days earlier as part of the all-sky VLBI survey yielded a correlated flux density of 1.4 Jy.

1215 − 457. An 18 mag quasar; $z = 0.529$; 2.3 GHz total flux density was 3.7 Jy. The source appears to be partially resolved on the VLA at 20 and 6 cm (Perley 1987). The SHEVE data show a slightly resolved 8 mas circular Gaussian component with flux density of 2.2 Jy. There were no SHEVE data on Hartebeesthoek baselines, but observations 2 yr earlier on a Tidbinbilla to Hartebeesthoek baseline at 2.3 GHz failed to detect the source with a detection limit of 0.1 Jy (Preston *et al.* 1985).

1322 − 427 (Centaurus A). A 7.0 mag S0 peculiar galaxy (NGC 5128) with a distinct dust lane; $z = 0.002$; nearest radio galaxy; 2.3 GHz total flux density was 1010 Jy. SHEVE data were obtained at both 2.3 and 8.4 GHz and are rich in structure. The details of the data analysis and the data for this source appear in a companion paper by Meier *et al.* (1989). The proposed model for the nuclear region consists of a compact core undetected at 2.3 GHz and a set of three knots spaced from 0.10″ to 0.16″ (2.5–4.0 pc) from the core and elongated along a position angle of 51°.

1409 − 651. A 9.4 mag Sb galaxy; $z = 0.0015$; 2.3 GHz total flux density was 1.3 Jy; 843 MHz map by us at Molonglo Observatory Synthesis Telescope shows complex structure 2′ in extent. Undetected on all baselines with an upper limit in correlated flux density of 0.03 Jy on the most sensitive baseline, Tidbinbilla to Parkes. However, since no calibration sources were observed with this source, we cannot be certain that all interferometer elements were functioning.

1421 − 490. Unidentified (crowded field); 2.3 GHz total flux density was 7.6 Jy with variations of less than 5% over preceding 12 yr. Australian SHEVE data were fitted by a pair of circular Gaussian sources with flux densities of 3.0 and 1.1 Jy and separated by 55 mas, with the stronger component at a position angle of 65° relative to the weaker one. No detection of the source on baselines to Hobart and Alice Springs indicates that each component must be at least 30 mas in diameter. The source was also not detected on baseline to Hartebeesthoek with a detection limit of 0.04 Jy.

1424 − 418. A 19 mag quasar (Jauncey 1986); $z = 1.522$ (Jauncey 1986); 2.3 GHz total flux density was 2.9 Jy with 50% variability on a 2 yr timescale. VLA data at 6 and 20 cm show extension along a position angle of − 10°. The Australian SHEVE data are well fitted to a pair of circular Gaussian sources with flux densities of 1.4 and 0.26 Jy, separated by 23 mas along a position angle of 56°. The stronger component is slightly extended (~5 mas); the other is unresolved. A large difference exists between the VLA and VLBI position angles (66°). The data on the Hartebeesthoek baselines indicate that the milliarcsecond nuclear structure has a minimum correlated flux density of 0.8 Jy and is more complex than a single symmetric component.

1516 − 569 (Circinus X-1). A flaring x-ray binary system in our galaxy. Observations were made during a weak flare and the source was only detected on the Tidbinbilla to Parkes baseline. The correlated flux density on this baseline matched the increase in the total flux density above the preflare level of about 0.3 Jy (see Fig. 7), indicating that the flaring component was unresolved and that the nonflaring component is totally resolved, which duplicates the results found by Preston *et al.* (1983 a) during another flare. The flaring component peaked at 0.2 Jy and decayed with a time constant of about 0.5 days. The nondetection of fringes in the period shortly after the flare start (not plotted) may be due to the failure of one of the interferometer elements, as no calibration sources were observed at this time.

1610 − 771. A 19 mag quasar; $z = 1.710$; 2.3 GHz total flux density was 5.4 Jy. Sparse Australian SHEVE data indicate a 3.8 Jy elliptical Gaussian core elongated 10 mas along a position angle of 35°, and a 1.4 Jy circular Gaussian halo about 50 mas in diameter. No data were obtained on baselines to Hartebeesthoek during the multibaseline coverage of this source, but data on the Hartebeesthoek–Tidbinbilla baseline taken a few days earlier as a part of the all-sky VLBI survey show that the milliarcsecond nuclear component had a minimum flux density of 0.9 Jy.

1718 − 649. A 12.6 mag spiral galaxy; $z = 0.014$; 2.3 GHz total flux density was about 4.5 Jy. The Australian SHEVE data are fitted equally well by several models comprised of a core and an extension at a position angle of $-65° \pm 20°$ with the extension separated from the core by about 15 mas. The model plotted includes a 4.0 Jy, 11 mas component elongated along a position angle of − 65° plus a 0.68 Jy point source offset by 17 mas along the same position angle. Data were obtained on only one baseline to Hartebeesthoek and indicate that the milliarcsecond nuclear structure has a minimum flux density of 0.5 Jy and is more complex than a circularly symmetric source.

1742 − 289 (Sagittarius A). The Galactic center; VLA observations indicate a three-armed spiral structure (Ekers *et al.* 1983). The analysis of these data is treated separately by Jauncey *et al.* (1989a) in a companion paper. The only SHEVE data are at 8.4 GHz on the Parkes–Tidbinbilla baseline and are fitted very well with a 1.2 Jy elongated Gaussian component 17×9 mas in size along a position angle of 82°. This probably represents a scattered image of the source, with the intrinsic source size being smaller.

1921 − 293 (OV − 236). A 17.5 mag quasar; $z = 0.352$; 2.3

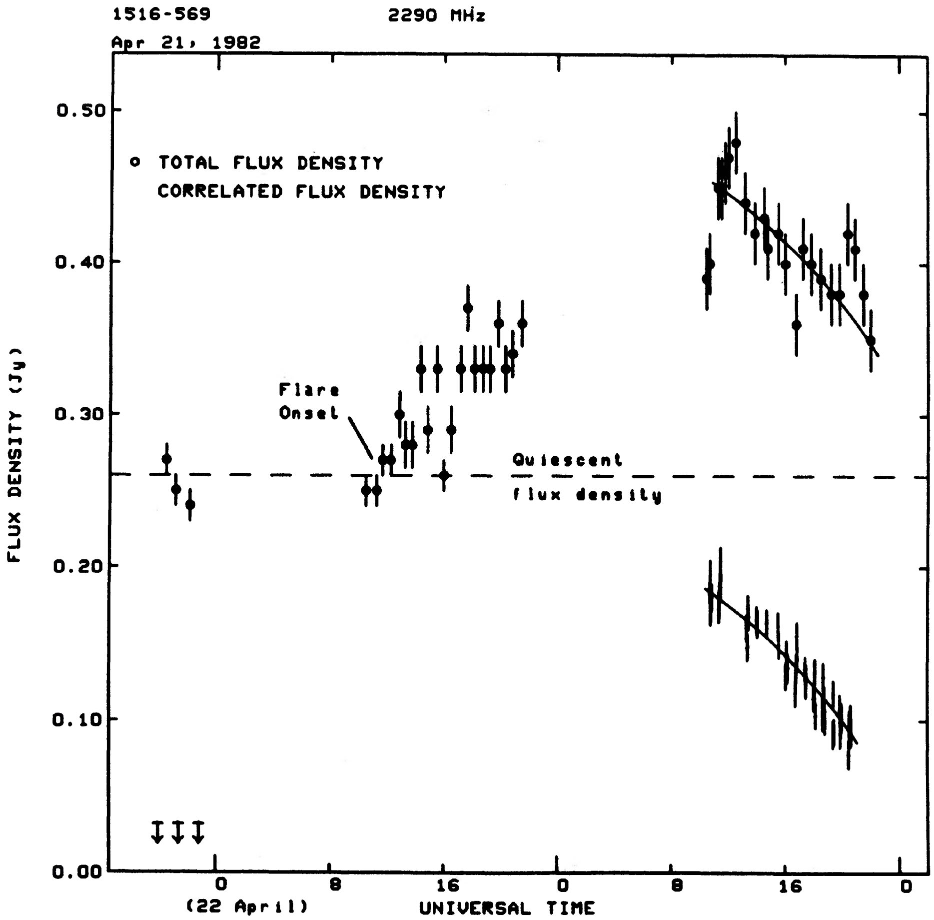

FIG. 7. Total and correlated flux density (DS43 – PRKS) of 1516 – 569 (Circinus X-1). The solid line in the plot of correlated flux densities represents the best-fit model. The solid line in the plot of total flux densities is the same model, with the quiescent total flux density added. Note that measured quiescent total flux density may be biased due to galactic background confusion.

GHz total flux density was about 6.5 Jy with 100% variability over a 1 yr timescale. The source was unresolved at the VLA at 6 and 20 cm. This source was slightly resolved with Australian SHEVE baselines and was fitted by a single elliptical Gaussian component with a flux density of 6.6 Jy and elongated 5 mas along a principal axis of about 25°. The baselines to Hartebeesthoek indicate that the milliarcsecond nuclear structure has a minimum flux density of 3.0 Jy.

1934–638. An 18.9 mag quasar; $z = 0.183$; 2.3 GHz total flux density was about 12.8 Jy with 10% variability over the preceding 15 yr. The SHEVE data and data analysis for this source appear in a separate companion paper by Tzioumis *et al.* (1989). The data are well fitted with a slightly unequal double source separated by 42 mas at a position angle of 90°, with a connecting bridge between the sources. Comparison with single-baseline data taken a decade earlier (Gubbay *et al.* 1971) indicate that the source structure has not changed. This source is a likely candidate for a Phillips–Mutel type double (Phillips and Mutel 1982).

2000–330. A 19 mag quasar; $z = 3.780$, the highest-redshift radio quasar known. A VLA map at a wavelength of 6 cm (Perley 1985) shows a small westward extension from the core. In Australia, the source was only observed on two short baselines, and appears unresolved, having a correlated flux density of 0.76 Jy. There were no data on Australia to Hartebeesthoek baselines, but 2.3 GHz observations 5 yr earlier on a similar-length baseline measured a correlated flux density of 0.5 Jy (Preston *et al.* 1985).

2203–188. A 19 mag quasar; $z = 0.618$; 2.3 GHz total flux density was about 5.8 Jy with less than 5% variability over the preceding 15 yr. VLA maps at 6 cm (Perley 1982, 1985) show a slight northward extension from the core at a position angle of about – 20°. We only detected the source on the small Tidbinbilla–Parkes–Fleurs triangle. Our data, primarily the phase-closure data, are best fitted by two circular Gaussian components with strengths of 2.9 and 0.84 Jy, with the weaker source separated from the stronger by 56 mas along a position angle of about 20°. The VLBI and VLA position angles differ by about 40°. Nondetection on the Tidbinbilla to Alice Springs baseline implies that the sizes of the strong and weak components are greater than about 12 and 20 mas, respectively. No data were obtained on Hartebeesthoek baselines, but Morabito *et al.* (1986) measured a 2.3 GHz correlated flux density of 0.07 Jy on a similar-length baseline six months earlier.

2245–328. An 18.6 mag quasar; $z = 2.268$; 2.3 GHz total flux density was 1.7 Jy and had dropped by 35% in the preceding 7 yr. The source was unresolved with the VLA at 6 and 20 cm. Both Australian and South African SHEVE data are well fitted by a circular Gaussian source of 1.7 Jy and 1.0 mas diameter. Unmodeled variations in the Hobart data are likely pointing errors.

2326–477. A 16.8 mag quasar; $z = 1.299$; 2.3 GHz total flux density was 2.8 Jy with about 10% variability over the preceding 11 yr. Australian SHEVE data indicate a point source at 2.6 Jy. The baselines to Hartebeesthoek indicate that the milliarcsecond nuclear structure is more complex than a single symmetric component and has a minimum flux density of 0.7 Jy.

2345 − 167. An 18 mag quasar; $z = 0.576$; 2.3 GHz total flux density was 3.2 Jy with 70% variability over a 2 yr timescale. A VLA map at 20 cm (Wardle, Moore, and Angel 1984) shows a 6″ extension from the core at position angle − 140°. The limited Australian SHEVE data are consistent with a 3.2 Jy, 11 mas elliptical Gaussian component elongated along a position angle of − 155°. VLBI and VLA position angles agree to within about 15°. The baselines to Hartebeesthoek indicate that the milliarcsecond nuclear structure has a minimum flux density of 1.9 Jy.

VII. SUMMARY

Six antennas in the southern hemisphere were operated as a VLBI array for a 2 week period. This experiment produced information on the fine-scale angular structure of 28 southern hemisphere radio sources. This VLBI array was temporary. However, it is planned that the Australia Telescope will eventually utilize several of the SHEVE sites (and perhaps other sites) as auxiliary elements to its base array. This would provide a permanent southern hemisphere instrument capable of achieving maps of better quality than SHEVE. In addition, future VLBI observatories in space (e.g., *Quasat*) will not necessarily need a large array of telescopes in the southern hemisphere to produce useful high-angular-resolution images in the south. The source maps produced by SHEVE should serve as a guide to source selection for such future space observatories.

The SHEVE experiment also provided precise astrometric positions of several radio sources, allowing the optical identification of many of them. Astrometric VLBI has continued to be carried out in the southern hemisphere since a large array of antennas is not necessary for this work. The future astrometric goals are to produce a high-precision radio reference frame in the far south, and tie it to similar existing frames farther north. Also, the radio reference frame in the far south will be linked to optical star-based reference frames.

The first accurate geodetic measurement of baselines with VLBI in the southern hemisphere was performed during the SHEVE experiment. VLBI geodetic measurements do not necessarily require a large array of antennas, and additional experiments in the southern hemisphere have already been performed.

Despite the temporary nature of the SHEVE array and limitations in its performance, significant new data have been obtained in radio-source structure, astrometry, and geodesy. This experiment will hopefully foster the further development of this valuable technique south of the equator.

Many people and organizations contributed to the success of the SHEVE experiment. In particular, we would like to thank Nick Renzetti (JPL) and Bob Frater (CSIRO) for their generous support and encouragement. We would also like to thank the Director, Tom Reid, and the staff at Tidbinbilla, the Director, Don Gray, and the staff of the Australian Landsat Facility at Alice Springs, and the Director and staff at the ANRAO, Parkes. Roy Livermore and Neil McVicar were particularly helpful at Tidbinbilla; Tim Pearson, Steve Unwin, and Richard Simon at Caltech provided assistance with analysis techniques; and Roland Taylor and Al Kirk from JPL tended the hydrogen maser at Parkes. The experiment would have been impossible without the support of the staffs of the Division of National Mapping, the CSIRO National Measurement Laboratories, and the Caltech/JPL Mark II Correlator. Rich Perley and Jim Ulvestad provided VLA results before publication, Warwick Wilson contributed to the initial installation at Alice Springs, Jim Roberts helped with the Parkes observations, and David Abreu helped with the Tidbinbilla observations. George Graves and the staff of the Fleurs Synthesis Telescope provided technical support.

Part of this research was carried out at the Jet Propulsion Laboratory of the California Institute of Technology, under contract to the National Aeronautics and Space Administration.

Anastasios Tzioumis acknowledges the receipt of a Commonwealth Postgraduate Award and support from the Science Foundation for Physics within the University of Sydney. Bruce Harvey acknowledges the receipt of a Commonwealth Postgraduate Award and was supported by the Rothmans Foundation.

REFERENCES

Antonucci, R. R. J., and Ulvestad, J. S. (1984). Astrophys. J. **294**, 158.
Cayatte, V., and Sol, H. (1987). Astron. Astrophys. **171**, 25.
Clark, B. G. (1973). Proc. IEEE **61**, 1242.
Cohen, M. H., Moffet, A. T., Romney, J. D., Schilizzi, R. T., Shaffer, D. B., Kellermann, K. I., Purcell, G. H., Grove, G., Swenson, G. W., Jr., Yen, J. L., Pauliny-Toth, I. I. K., Preuss, E., Witzel, A., and Graham, D. (1975). Astrophys. J. **201**, 249.
Cristiani, S. (1985). IAU Circ. No. 4027.
Danziger, I. J., Fosbury, R. A. E., Goss, W. M., and Ekers, R. D. (1979). Mon. Not. R. Astron. Soc. **188**, 415.
Danziger, I. J., Shaver, P. A., Moorwood, A. F. M., Fosbury, R. A. E., Goss, W. M., and Ekers, R. D. (1985). ESO Messenger **39**, 20.
Ekers, R. D., van Gorkom, J., Schwarz, U. J., and Goss, W. M. (1983). Astron. Astrophys. **122**, 143.
Gubbay, J. S., Legg, A. J., and Robertson, D. S. (1972). Aust. J. Phys. **25**, 461.
Gubbay, J. S., Legg, A. J., Robertson, D. S., Craske, N., and Nicolson, G. D. (1971). Astron. J. **76**, 965.
Gubbay, J. S., Legg, A. J., Robertson, D. S., Nicolson, G. D., Moffet, A., and Shaffer, D. (1977). Astron. J. **215**, 20.
Harvey, B. R., Stolz, A., Niell, A. E., Morabito, D., Preston, R. A., and Jauncey, D. L. (1983). Aust. J. Geod. Photo Surv. **38**, 39.
Jauncey, D. L. (1986). Private communication.
Jauncey, D. L., *et al.* (1989a). Astron. J. **98**, 44.
Jauncey, D. L., *et al.* (1989b). Astron. J. **98**, 49.
Jauncey, D. L., *et al.* (1989c). Astron. J. **98**, 54.
Keel, W. C. (1986). Astrophys. J. **302**, 296.
Meier, D. L., *et al.* (1989). Astron J. **98**, 27.
Morabito, D. D., Niell, A. E., Preston, R. A., Linfield, R. P. Wehrle, A. E., and Faulkner, J. (1986). Astron. J. **91**, 1038.
Morabito, D. D., Preston, R. A., Linfield, R. P., Slade, M. A., and Jauncey, D. L. (1986). Astron. J. **92**, 546.
Perley, R. (1982). Astron. J. **87**, 859.
Perley, R. (1985). Private communication.
Perley, R. (1987). Private communication.
Phillips, R. B., and Mutel, R. L. (1982). Astron. Astrophys. **106**, 21.

Preston, R. A., Jauncey, D. L., Tzioumis, A., Meier, D. L., Skjerve, L. J., Ables, J., Batchelor, R., Faulkner, J., Hamilton, P. M., Haynes, R., Johnson, B., Louie, A., McCulloch, P., Moorey, G., Morabito, D. D., Nicolson, G., Neill, A. E., Robertson, J. G., Royle, G. W. R., Slade, M. A., Slee, O. B., Watkinson, A., Wehrle, A. E., and Wright, A. (1984). In *VLBI and Compact Radio Sources*, IAU Symposium No. 110, edited by R. Fanti, K. Kellerman, and G. Setti (Reidel, Dordrecht), p. 67.

Preston, R. A., Morabito, D. D., Wehrle, A. E., Jauncey, D. L., Batty, M. J., Haynes, R. F., Wright, A. E., and Nicolson, G. D. (1983a). Astrophys. J. Lett. **268**, L23.

Preston, R. A., Wehrle, A. E., Morabito, D. D., Jauncey, D. L., Batty, M. J., Haynes, R. F., Wright, A. E., and Nicolson, G. D. (1983b). Astrophys. J. Lett. **266**, L93.

Preston, R. A., Morabito, D. D., Williams, J. G., Faulkner, J., Jauncey, D. L., and Nicolson, G. D. (1985). Astron. J. **90**, 1599.

Readhead, A. C. S., and Wilkinson, P. N. (1978). Astrophys. J. **223**, 25.

Schwab, F. R., and Cotton, W. D. (1983). Astron. J. **88**, 688.

Stolz, A., Harvey, B., Jauncey, D. L., Niell, A., Morabito, D., Preston, R., Greene, B., Lambeck, K., Tzioumis, A., Watkinson, A., Royle, G. W. R., and Johnson, D. (1983). Aust. Surveyor **31**, 305.

Tzioumis, A. K. (1985). In *20th International Electronics Convention and Exhibition of the Institution of Radio and Electronics Engineers Australia Digest of Papers* (IREE, Sydney), p. 607.

Tzioumis, A. K. (1987). Ph. D. thesis, The University of Sydney.

Tzioumis, A. K. *et al.* (1989). Astron. J. **98**, 36.

Ulvestad, J., Johnston, K., Perley, R., and Fomalont E. (1981). Astron. J. **86**, 1010.

Wardle, J. F. C., Moore, R. L., and Angel, J. R. P. (1984). Astrophys. J. **279**, 93.

THE ASTRONOMICAL JOURNAL

FOUNDED BY B. A. GOULD
1849

VOLUME 98 — July 1989 ~ No. 1602 — NUMBER 1

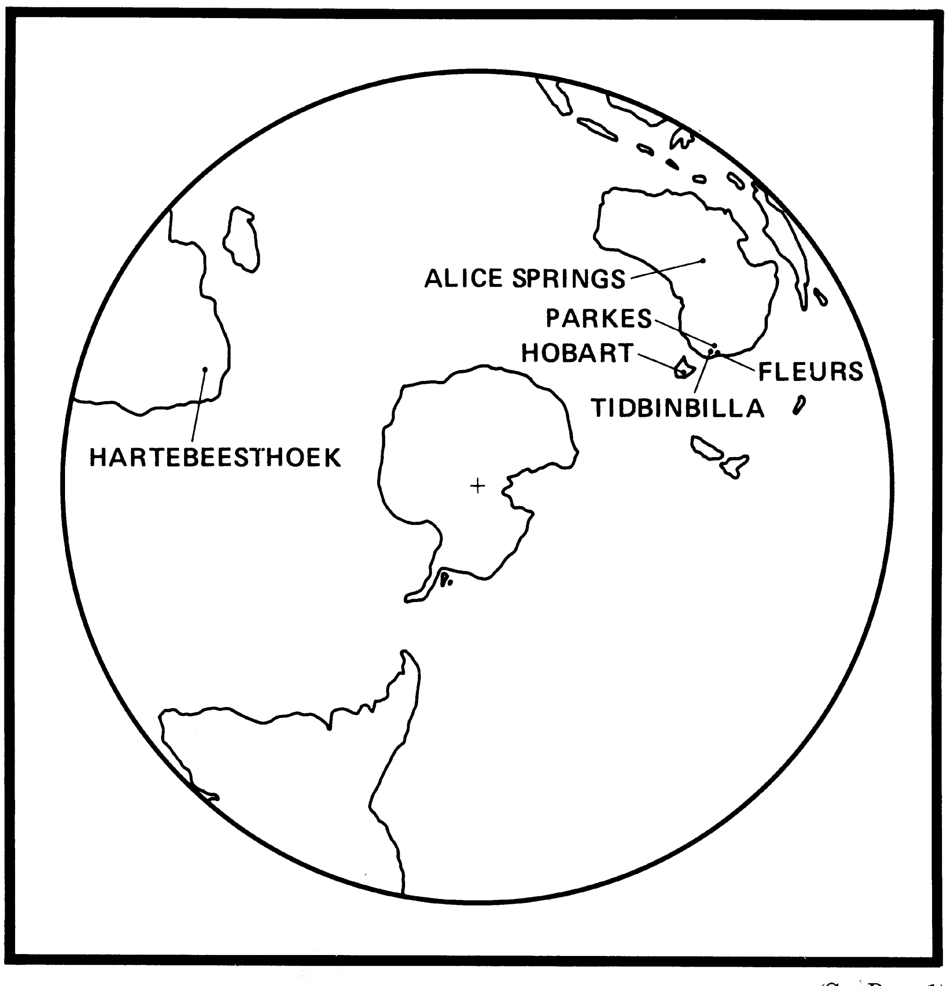

(See Page 1)

Published for the
AMERICAN ASTRONOMICAL SOCIETY
by the
AMERICAN INSTITUTE OF PHYSICS